Theory Manual

Release 1.0.0

Morphorm

Jan 18, 2025

INTRODUCTION

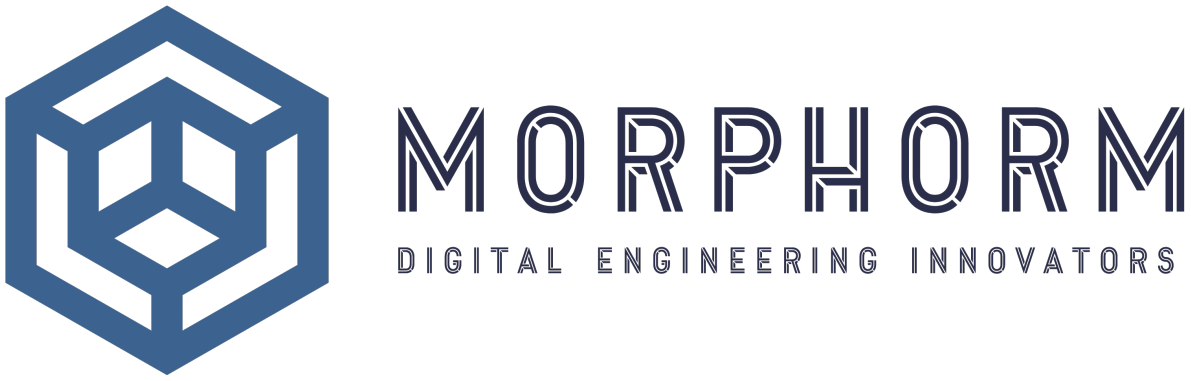

These pages are meant to serve as the `Theory Manual` for the Morphorm Software.

CHAPTER

ONE

INTRODUCTION

descriptionThe *Introduction* chapter describes the Morphorm digital engineering ecosystem and some of the general concepts used to derive the simulation-driven design formulations.

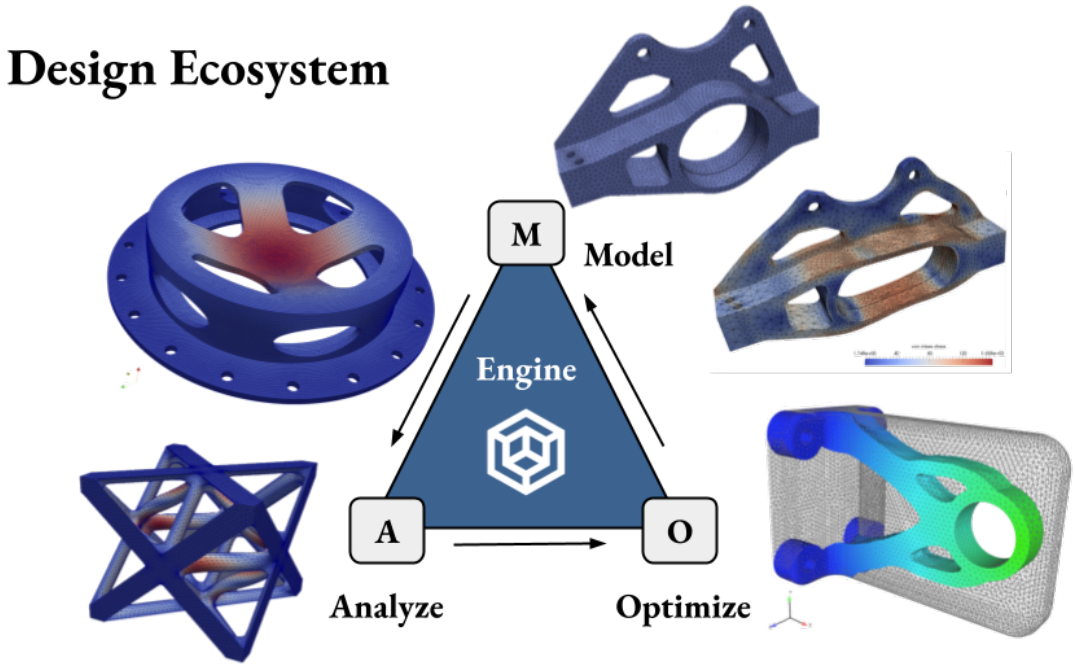

Fig. 1.1: The Morphorm design ecosystem is comprised by four high level modules: (1) Analyze, (2) Model, (3) Optimize, and (4) Engine. The Analyze module predicts how a physical system interacts with its environment by numerically solving the differential equations governing the behavior of the system. The Model module constructs a geometry model of the physical system under investigation. The Optimize module applies optimization methods to optimized the performance, reliability, and efficiency of the physical system. The Engine module facilitates automated exchange of information between the analysis, modeling, optimization, and other performers; e.g., third-party application, at runtime. Given multiple environments; i.e., boundary conditions of interests, the Engine applies a Multiple Program, Multiple Data parallel model to facilitate concurrent evaluations of the physical system.

1.1 Description

Morphorm builds modeling, simulation, and optimization technologies to deliver real-time design solutions. Our mission is to employ advanced scientific computing to solve complex science and engineering problems. We aspire to be the most innovative digital engineering company, where our clients can discover in real-time design solutions.

Our products exploit distributed memory parallel programming models and performance portability to optimally perform large-scale calculations on heterogeneous and homogeneous computing systems. The Morphorm platform, Fig. 1.1, includes tools for multiphysics finite element analysis, design optimization, immersed modeling methods, and uncertainty quantification and propagation, and much more.

1.2 General Concepts

1.2.1 Partial Differential Equations

Lets consider a real-valued function $u(x, y)$ of two independent real variables x and y. A second-order, linear, constant-coefficient partial differential equation for $u(x, y)$ is defined as:

$A\frac{\partial^2 u}{\partial x^2} + 2B\frac{\partial^2 u}{\partial x \partial y} + C\frac{\partial^2 u}{\partial y^2} + D\frac{\partial u}{\partial x} + E\frac{\partial u}{\partial y} + F = 0.$

The quantities x and y usually represent position and time, respectively [Evans]. A partial differential equation (PDE) is classified as *elliptic* if the coefficients of the terms containing the second derivatives of u satisfy the condition $B^2 - AC < 0$. The simplest example of a second-order linear elliptic PDE is the Laplace equation:

$\Delta u = 0.$

A PDE is classified as *parabolic* if the coefficients of the terms containing the second derivatives of u satisfy the condition $B^2 - AC = 0$. The simplest example of a parabolic PDE is the heat equations, which has the form:

$\frac{\partial u}{\partial t} - \alpha\frac{\partial^2 u}{\partial x^2} = 0,$

where $u(x, t)$ is the temperature at position x in the body at time t and α is a positive constant called the thermal diffusivity.

A PDE is classified as *hyperbolic* if the coefficients of the terms containing the second derivatives of u satisfy the condition $B^2 - AC > 0$. An example of a hyperbolic PDE is the wave equation:

$\frac{\partial^2 u}{\partial t^2} - c^2\frac{\partial^2 u}{\partial x^2} = 0,$

where $u(x, t)$ is a scalar field representing the conserved quantity at position x in the body at time t, e.g., pressure. The positive real-valued constant c^2 represents the propagation speed of the wave.

1.2.2 Newton-Raphson

The Newton-Raphson method, also known as Newton's method, is a root-finiding algorithm capable of successively producing better approximations to the roots of a real-valued function [Golub and Van Loan] [Nocedal and Wright]. The Newton-Raphson method is foundational to solving the governing equations describing physical systems. Indeed, let X and Y be two vector spaces and $\mathbf{F}\colon X \to Y$ be Frechet differentiable, given an initial datum $\mathbf{u}^0 \in X$ and tolerance $tol > 0$, solve the following linear system of equations:

$$\begin{aligned} \mathbf{J}\left(\mathbf{u}^k\right)\delta\mathbf{u}^k &= -\mathbf{F}\left(\mathbf{u}^k\right) \\ \mathbf{u}^{k+1} &= \mathbf{u}^k + \delta\mathbf{u}^k \end{aligned} \tag{1.2.1}$$

until $\|\mathbf{F}\left(\mathbf{u}^{k+1}\right)\|_Y < tol$. The $(i, j) - th$ entry of the Jacobian matrix $\mathbf{J}$ is defined as the Frechet derivative of the $i - th$ row of $\mathbf{F}$ with respect to the $j - th$ variable. See [Ortega and Rheinboldt] for the convergence analysis of the Newton-Raphson.

1.3 User Support

You can submit questions via email to help@morphorm.com.

CHAPTER

TWO

PHYSICS

The *Physics* chapter presents the governing equations implemented in the Morphorm software to simulate the behavior of physical systems with the finite element method.

2.1 Thermal

2.1.1 Heat Equation

The energy balance equation state that the rate of change of thermal energy equals the sum of the heat generated by internal thermal sources and the heat that flows into the body through the boundaries. Mathematically, this statement is expressed as:

$$\int_{\Omega} \rho \frac{\partial U}{\partial t} \, d\Omega = \int_{\Gamma} \mathbf{q} \cdot \mathbf{n} \, d\Gamma + \int_{\Omega} H \, d\Omega, \tag{2.1.1}$$

where t denotes time and Ω is a volume of solid material with boundary Γ. The parameter ρ is the material density. The material time rate of internal energy $\partial U/\partial t$ is defined as:

$$\frac{\partial U}{\partial t} = c_p \frac{\partial \theta}{\partial t}, \tag{2.1.2}$$

where the specific heat capacity c_p (at constant pressure in the case of a gas) is the amount of heat to be supplied to an object to produce a unit change in its temperature θ. The heat flux $\mathbf{q}$ is the incoming heat flux per unit area of the body, where $\mathbf{n}$ is the outward unit normal to boundary Γ. Finally, H is the heat generated per unit time per unit volume at position $\mathbf{x}$, i.e., heat source. The lowercase bold notation is used in this manuscript for vector quantities.

The divergence theorem is applied to transform the boundary flux integral in Eq.2.1.1 into a volume integral of the form:

$$\int_{\Gamma} \mathbf{q} \cdot \mathbf{n} \, d\Gamma = \int_{\Omega} \nabla \cdot \mathbf{q} \, d\Omega. \tag{2.1.3}$$

Substituting Eq.2.1.3 into Eq.2.1.1 gives:

$$\int_{\Omega} \rho \frac{\partial U}{\partial t} \, d\Omega = \int_{\Omega} \nabla \cdot \mathbf{q} \, d\Omega + \int_{\Omega} H \, d\Omega, \tag{2.1.4}$$

where material time rate of internal energy is defined by Eq.2.1.2. Since Ω is arbitrary, if Eq.2.1.4 is smooth enough, the energy balance equation is equivalent to:

$$\rho \frac{\partial U}{\partial t} - \nabla \cdot \mathbf{q} = H. \tag{2.1.5}$$

2.1.2 Constitutive Relation

There are two unknowns in Eq.2.1.5, the temperature θ and the heat flux $\mathbf{q}$, and only one equation. A second equation is required to fully characterize the behavior of the physical system. If heat conduction is assumed to be governed by Fourier's law, which states that the heat flux is linearly related to the temperature gradient as [Callen]:

$$\mathbf{q} = -k\nabla\theta, \tag{2.1.6}$$

where $\nabla\theta$ is the temperature gradient with respect to spatial coordinate $\mathbf{x}$ and the constant k is the thermal conductivity[1]. The minus sign in Eq.2.1.6 signals that heat flows from hot to cold regions.

2.1.3 Nondimensional Form

The dimensions of the parameters in Eq.2.1.5 is a combination of the following fundamental dimensions: length (L), time (T), mass (M), and temperature (Θ). The scaling factors use to remove the dimensions from Eq.2.1.5 are given in Table 2.1.1.

Table 2.1.1: Scaling factors for the heat equation.

Symbol	Description	Scaling Factor	Units
x_i	i-th spatial coordinate	x_o	L
θ	temperature	θ_o	Θ
t	time	x_o^2/k_o	$MLT^{-3}\Theta^{-1}$
k	thermal conductivity	k_o	$[energy]L^{-1}\Theta^{-1}$
e	energy	e_o	ML^2T^{-3}

The characteristic length x_o is chosen such that it is of the same order of magnitude as the diameter of the computational domain Ω:

$$x_o = O(\text{diam}(\Omega)). \tag{2.1.7}$$

The characteristic temperature θ_o is choosen such that it corresponds to the maximum value from all the Dirichlet temperature values. This scaling facilitates the scaled temperature at Dirichlet boundary conditions to be maximally of the order of magnitude 1.0. Therefore, substituting the scaling factors tabulated in Table 2.1.1 into Eq.2.1.5 gives:

$$\frac{\partial\widehat{\theta}}{\partial\widehat{t}} = \nabla\cdot\left(\nabla\widehat{\theta}\right) + \lambda_\theta H, \tag{2.1.8}$$

where the scaling parameter λ_θ is defined as:

$$\lambda_\theta = \frac{x_o^2}{\theta_o k_o}. \tag{2.1.9}$$

The hat notation is used to specify a scaled variable.

2.1.4 Weak Form

Let $H^1(\Omega)$ be the Sobolev space of weakly differentiable functions and $H_D^1(\Omega) = \{w \in H^1(\Omega) | w = 0 \text{ on } \Gamma_D\}$, with Γ_D defined as the Dirichlet boundary. The variational form of the heat equation intorduced in Eq.2.1.5 is defined as:

$$\int_\Omega \rho\frac{\partial U}{\partial t} w\, d\Omega - \int_\Omega (\nabla\cdot\mathbf{q})\, w\, d\Omega = \int_\Omega Hw\, d\Omega. \tag{2.1.10}$$

Applying the product rule and then the divergence theorem to Eq.2.1.10 gives:

$$\int_\Omega \rho\frac{\partial U}{\partial t} w\, d\Omega + \int_\Omega \mathbf{q}\nabla w\, d\Omega = \int_\Omega Hw\, d\Omega + \int_\Gamma q_0 w\, d\Gamma, \tag{2.1.11}$$

[1] The thermal conductivity property can be anisotropic.

where q_0 denotes the flux normal to the boundary. If the problem does not depend on time, the steady state form for the variational for of the heat equation is derived, which is defined as:

$$\int_\Omega (\kappa \nabla \theta) \nabla w \, d\Omega - \int_\Omega H w \, d\Omega - \int_\Gamma q_0 w \, d\Gamma = 0, \tag{2.1.12}$$

where the heat flux $\mathbf{q} = -\kappa \nabla \theta$ was replaced with Fourier's law. Notice that the thermal conductivity constant k is replace with the thermal diffusivity constant $\kappa = k/c_v$, where $c_v = \rho c_p$ is the volumetric heat capacity[2]. The variational forms of the unsteady and steady nondimensional heat equation follow analogously.

2.1.5 Boundary Conditions

Boundary conditions can be specified as:

- a prescribed temperature $\theta = \theta(\mathbf{x}, t)$
- a prescribed surface heat flux $q_0 = q_0(\mathbf{x}, t)$ per unit area
- a prescribed volumetric heat source $H = H(\mathbf{x}, t)$ per unit volume
- surface convection $q_c = q_c(\mathbf{x}, t) = h\,(\theta - \theta_0)$, where $h = h(\mathbf{x}, t)$ is the heat transfer coefficient and $\theta_0 = \theta_0(\mathbf{x}, t)$ is the sink temperature.

If the problem does not depend on time (steady state thermal problem), time is set to zero, i.e., $t = 0$.

2.1.6 Optimization

The gradient of a nonlinear design criterion with respect to the vector design variables $\mathbf{z}$ is computed using the solution method for elliptic partial differential equations presented in the *Optimization* chapter, subsection *Elliptic*.

2.2 Electrical

The Electrical Module allows the user to solve different sets of partial differential equations, incuding the Poisson/Laplace equation, the drift-diffusion continuity equations for electrons and holes, and the lattice temperature equation. Some of the partial differential equations can be solved individually or coupled based on the intended application.

2.2.1 Laplace Equation

The electric field in a conductive material is governed by Maxwell's equation of conservation of charge [Sze *et al.*]. Assuming steady-state direct current, the equation reduces to:

$$\int_\Gamma \mathbf{J} \cdot \mathbf{n} \, d\Gamma = \int_\Omega R_c \, d\Omega, \tag{2.2.1}$$

where Ω is the control volume whose surface is Γ, $\mathbf{n}$ is the outward normal vector to Γ, $\mathbf{J}$ is the electric current density (current per unit area), and R_c is the internal current source per unit volume.

The divergence theorem is used to convert the surface integral in Eq.2.2.1 into a volume integral of the form:

$$\int_\Omega \left(\nabla \cdot \mathbf{J} - R_c\right) \, d\Omega = 0, \tag{2.2.2}$$

where ∇ denotes the gradient operator. Since the volume Ω is arbitrary, Eq.2.2.2 provides the following pointwise differential equation describing the steady state behavior of an electrical device:

$$\nabla \cdot \mathbf{J} - R_c = 0. \tag{2.2.3}$$

[2] The thermal diffusivity property can be anisotropic.

Weak Formulation

Let $H^1(\Omega)$ be the Sobolev space of weakly differentiable functions and $H^1_D(\Omega) = \{w \in H^1(\Omega) | w = 0 \text{ on } \Gamma_D\}$, with Γ_D defined as the Dirichlet boundary. The weak form of Eq.2.2.3 is obtained by introducing an arbitrary, variational electric potential field w and integrating over the volume Ω as follows:

$$\int_\Omega w \left(\nabla \cdot \mathbf{J} - R_c\right) \, d\Omega = 0. \tag{2.2.4}$$

Applying the product rule to reduce the derivative order on an expression in conjunction with the divergence theorem, Eq.2.2.4 is recast as:

$$-\int_\Omega \nabla w \cdot \mathbf{J} \, d\Omega = \int_\Gamma w J_0 \, d\Gamma + \int_\Omega w R_c \, d\Omega, \tag{2.2.5}$$

where $J_0 = -\mathbf{J} \cdot \mathbf{n}|_\Gamma$ is the current density entering the control volume across the boundary Γ.

Constitutive Relation

The flow of electric current is described by Ohm's law as:

$$\mathbf{J} = \epsilon_0 \epsilon_r \mathbf{E}, \tag{2.2.6}$$

where ϵ_0 is the vacuum permittivity and ϵ_r is the relative permittivity or dielectric constant of a material. The electric field $\mathbf{E}$ is defined as the gradient of the electric potential ψ, which is defined as:

$$\mathbf{E} = -\nabla \psi, \tag{2.2.7}$$

where ψ is the electric potential. Since a potential rise occurs when a charge particle moves against the electric field, the direction of the gradient is opposite to that of the electric field. Using this definition for the electric field, Ohm's law is recast as:

$$\mathbf{J} = -\epsilon_0 \epsilon_r \nabla \psi. \tag{2.2.8}$$

The current density $\mathbf{J}$ is replaced with Eq.2.2.8 in Eq.2.2.5.

Electro-thermostatics

The following solution strategy is used to solve for the temperature and the electric potential of an electrical device subjected to thermally- and electrically-induced excitations:

1. Solve the *electrostatics equation*:

   $\mathbf{R}_\psi = \int_\Omega \nabla w \left(\epsilon_0 \epsilon_r \nabla \psi\right) \, d\Omega - \int_\Gamma w J_0 \, d\Gamma - \int_\Omega w R_c \, d\Omega = 0 \quad \in H^1(\Omega),$

   for the electrical potential $\psi \in H^1(\Omega)$, and

2. Solve the thermostatics equation:

   $\mathbf{R}_\theta = \int_\Omega \nabla w \left(\kappa \nabla \theta\right) \, d\Omega - \int_\Omega w H \, d\Omega - \int_\Gamma w q_0 \, d\Gamma = 0 \quad \in H^1(\Omega),$

   for the temperature $\theta \in H^1(\Omega)$.

The heat generation in the electrically conductive medium is coupled to the thermostatics equation Eq.2.1.12 through the heat generation rate $H = H_\theta + H_\psi$. The heat generation rate is decomposed into a termally-induced heat source H_θ and an *electrically-induced heat source* H_ψ.

Joule Heating

The flow of current through an electrical conductor produces thermal energy. This physical process is known as Joule heating. Mathematically, Joule heating is defined as:

$$H_J = \mathbf{J} \cdot \mathbf{E} \tag{2.2.9}$$

where $\mathbf{J}$ is the current density and $\mathbf{E}$ is the electric field. Multiplying Eq.2.2.9 by the variational temperature field w and integrating over the volume gives the weak form for the Joule heating source term:

$$H_J = \int_\Omega w \left(\mathbf{J} \cdot \mathbf{E}\right) \, d\Omega. \tag{2.2.10}$$

Substituting the Joule heating expression into Eq.2.1.12 gives:

$$\mathbf{R}_\theta = \int_\Omega \nabla w \left(\kappa \nabla \theta\right) \, d\Omega - \int_\Omega w H_\theta \, d\Omega - \int_\Omega w H_\psi \, d\Omega - \int_\Gamma w q_0 \, d\Gamma = 0, \tag{2.2.11}$$

where H_ψ is defined by Eq.2.2.9.

Boundary Conditions

Boundary conditions for electrostatic physics can be specified as:

- a prescribed electric potential $\psi = \psi(\mathbf{x}, t)$
- a prescribed boundary current density $J_0 = J_0(\mathbf{x}, t)$ per unit area,
- a prescribed thermal source $H = H(\mathbf{x}, t)$ per unit volume, which is decomposed into a thermally-induced heat source H_θ and an electrically-induced heat source H_J.

In addition to the boundary conditions listed above for electrostatic physics, the following boundary conditions can be specified for electro-thermostatic physics:

- a prescribed temperature $\theta = \theta(\mathbf{x}, t)$
- a prescribed surface heat flux $q_0 = q_0(\mathbf{x}, t)$ per unit area
- convective heat transfer on surface Γ_c, which is defined as:

  $q_c = q_c(\mathbf{x}, t) = h \left(\theta - \theta_0\right)$,

  where $h = h(\mathbf{x}, t)$ is the heat transfer coefficient and $\theta_0 = \theta_0(\mathbf{x}, t)$ is the sink temperature.

If the problem does not depend on time (steady state physics), time is set to zero, i.e., $t = 0$.

Optimization

The gradient of a nonlinear design criterion with respect to the vector design variables $\mathbf{z}$ is computed using the solution method for elliptic partial differential equations presented in the *Optimization* chapter, subsection *Elliptic*. The solution method applies to both electrostatics and thermo-electrostatics physics.

2.2.2 Van Roosbroeck Equations

The basic semiconductor device equations were derived for the first time by Van Roosbroeck [Van Roosbroeck]. A semiconductor device occupies a bounded, simply connected domain Λ in $\mathbb{R}^d$, where $d \in 1, 2, 3$ denotes the spatial dimension. It consists of a semiconductor part occupying the subdomain $\Omega \subseteq \Lambda$, and in the case of a metal-oxide -semiconductor device, of one or more oxide domains $\Phi = \bigcup_{i=1}^{N_\Phi} \Phi_i$, where N_Φ is the number of oxide domains. Thus, a typical semiconductor device is the union of its semiconductor and oxide subdomains, i.e., $\Lambda = \Omega \cup \Phi$. For a pure semiconductor device $\Lambda = \Omega$ and $\Phi = \emptyset$ holds [Markowich].

The Van Roosbroeck equations can be derived from Maxwell's equations [Sze *et al.*]:

$$\nabla \times \mathbf{E} = -\frac{\partial \mathbf{B}}{\partial t} \quad \text{(Faraday's law)}, \tag{2.2.12}$$

$$\nabla \times \mathbf{H} = \mathbf{J}\frac{\partial \mathbf{D}}{\partial t} \quad \text{(Ampere's law)}, \tag{2.2.13}$$

$$\nabla \cdot \mathbf{D} = \varrho \quad \text{(Gauss' law)}, \tag{2.2.14}$$

$$\nabla \cdot \mathbf{B} = 0 \quad \text{(no magnetic monopole)}, \tag{2.2.15}$$

$\mathbf{E}$ and $\mathbf{D}$ are the electric field and displacement vectors, respectively. $\mathbf{H}$ and $\mathbf{B}$ are the magnetic field and induction vectors, respectively. $\mathbf{J}$ is the conduction current density and ϱ is the electric charge density. The vector $\mathbf{x} \in \mathbb{R}^d$ denotes a spatial coordinate and $t \geqq 0$ is the time variable. The electric field is and the electric displacement related are related by:

$$D_i = \epsilon_{ij} E_j \quad \text{for} \quad i, j \in \{1, 2, 3\}, \tag{2.2.16}$$

where ϵ is the second order permittivity tensor of the medium. The permittivity is assumed to be time-independent and spatially homogeneous in Λ, i.e., $\epsilon_{ij} = \epsilon I_{ij}$, where I_{ij} is the second order identity tensor. The constant $\epsilon = \epsilon_r \epsilon_0$ is the absolute permittivity, where ϵ_r is the relative permittivity of the medium and ϵ_0 is the vacuum permittivity.

Poisson's Equation

Eq.2.2.15 can be satisfied by the following vector potential:

$$\mathbf{B} = \nabla \times \mathbf{A} \tag{2.2.17}$$

where it is clear that for a given magnetic induction vector $\mathbf{B}$, the vector potential $\mathbf{A}$ is not uniquely defined. The expression for the divergence of $\mathbf{A}$ will be defined later. For now, Eq.2.2.17 is inserted into Eq.2.2.15, which gives:

$$\nabla \times \left(\mathbf{E} + \frac{\partial \mathbf{A}}{\partial t} \right). \tag{2.2.18}$$

A sufficiently smooth vortex-free vector field defined in a simply connected domain is a dradient field. Thus, the electric field is defined as:

$$\mathbf{E} = -\frac{\partial \mathbf{A}}{\partial t} - \nabla \psi, \tag{2.2.19}$$

where ψ is a scalar potential. Substituting Eq.2.2.19 for $\mathbf{E}$ in Eq.2.2.16 gives:

$$\mathbf{D} = \epsilon \left(-\frac{\partial \mathbf{A}}{\partial t} - \nabla \psi \right) \tag{2.2.20}$$

Next, Eq.2.2.20 is inserted into Eq.2.2.14, which gives:

$$\epsilon \frac{\partial}{\partial t} \nabla \cdot \mathbf{A} + \epsilon \Delta \psi = -\varrho. \tag{2.2.21}$$

In order to make Eq.2.2.21 invariant under the Lorentz transformation [Hofmann],

$$\nabla \cdot \mathbf{A} = -\frac{1}{c^2} \frac{\partial \psi}{\partial t}, \tag{2.2.22}$$

where c denotes the speed of light in vacuum with a constant numerical value of $2.99792458 \times 10^{10} \mathrm{cm} \cdot \mathrm{s}^{-1}$. Inserting Eq.2.2.22 into Eq.2.2.21 gives:

$$-\frac{\epsilon}{c^2} \frac{\partial^2 \psi}{\partial t^2} + \epsilon \Delta \psi = -\varrho, \tag{2.2.23}$$

which is the wave equation. The speed of light in vacuum is normally assumed to be larger than the characteristic propagation velocities in a semiconductor device. Therefore, the second-order time derivative (wave-propagation term) is neglected and Poisson's equation for the electric potential ψ is derived:

$$\epsilon\Delta\psi = -\varrho \tag{2.2.24}$$

The electric charge density ϱ in semiconductor device applications is written as:

$$\varrho = q\left(p - n + C\right), \quad \mathbf{x} \in \Omega, \tag{2.2.25}$$

where q is the elementary charge, which takes a constant numerical value of $1.6021892 \times 10^{-19}\mathrm{A}\cdot\mathrm{s}$. The concentration of (positively charged) holes is denoted with p and the concentration of (negatively charged) conduction electrons is denoted with n. The profile of electrically active deposits is denoted with C, which is defined as:

$$C = N_D^+ - N_A^-, \quad \mathbf{x} \in \Omega \tag{2.2.26}$$

under the usual assumption that all impurity atoms are singly ionised. The concentration of electrically active donor atoms and the concentration of electrically active acceptor atoms is denoted by N_D^+ and N_A^-, respectively.

It is conventional to assume that the oxide subdomains are charge-neutral, i.e., $\varrho = 0$, $\mathbf{x} \in \Phi$. Thus, Eq.2.2.24 (Poisson's equation) is only evaluated in the semiconductor device, i.e.,

$$-\epsilon\Delta\psi = \begin{cases} q\left(p - n + C\right), & \mathbf{x} \in \Omega \\ 0, & \mathbf{x} \in \Phi \end{cases} \tag{2.2.27}$$

Continuity Equations

Applying the divergence operator to Eq.2.2.13 and using Eq.2.2.14 gives:

$$0 = \nabla \cdot \mathbf{J} + \frac{\partial \varrho}{\partial t}, \tag{2.2.28}$$

where the property $\nabla \cdot (\nabla \times \mathbf{H}) = 0$ was used to derive Eq.2.2.28. Therefore, sources and sinks of the conduction current density and solely determined by the temporal variation of the charge density.

The conduction current density is split into contributions from the electron current density $\mathbf{J}_n$ and the hole current density $\mathbf{J}_p$, i.e.,

$$\mathbf{J} = \mathbf{J}_n + \mathbf{J}_p. \tag{2.2.29}$$

Substituting Eq.2.2.29 into Eq.2.2.28 gives:

$$-\nabla \cdot \mathbf{J}_p - q\frac{\partial p}{\partial t} = \nabla \cdot \mathbf{J}_n - q\frac{\partial n}{\partial t}, \quad \mathbf{x} \in \Omega, \tag{2.2.30}$$

where charge defects have been neglected in Eq.2.2.30, i.e., $\frac{\partial C}{\partial t} = 0$ [Selberherr]. The equations for the electron and hole current densities are derived from Eq.2.2.30 by settings both sides equal to the quantity qR, i.e.,

$$\nabla \cdot \mathbf{J}_n - q\frac{\partial n}{\partial t} = qR, \quad \mathbf{x} \in \Omega. \tag{2.2.31}$$

$$-\nabla \cdot \mathbf{J}_p - q\frac{\partial p}{\partial t} = qR, \quad \mathbf{x} \in \Omega. \tag{2.2.32}$$

The quantity R is referred as the recombination-generation rate. The recombination-generation rate is defined as the difference of the rate at which electron-hole carrier pairs recombine and the rate at which they are generated in the semiconductor Ω. If $R < 0$ generation prevails in Ω and if $R > 0$ recombination prevails. The oxide is assumed to be an ideal insulator, i.e., $\mathbf{J}_n|_\Phi \equiv \mathbf{J}_p|_\Phi \equiv 0$.

Current Density Equations

The two main sources for current flow in a semiconductor device are: (1) diffusion of the electron and hole ensembles and (2) drift of electrons and holes caused by the electric field as driving force. The main assumption used to derive the expressions for the carrier current densities is that the carrier current flows are determined by linearly superimposing the diffusion and the drift processes as follows:

$$\mathbf{J}_n = \mathbf{J}_n^{\text{diff}} + \mathbf{J}_n^{\text{drift}}, \quad \mathbf{J}_p = \mathbf{J}_p^{\text{diff}} + \mathbf{J}_p^{\text{drift}} \tag{2.2.33}$$

Electrons and holes diffuse from regions with high concentration into regions with low concentrations.

The direction of diffusion of a particle ensemble is the direction of steepest descent of the corresponding particle concentration. Furthermore, by Fourier's law, the diffusion flux densities are proportional to the gradients of the corresponding particle concentration [Lin and Segel], i.e.,

$$\mathbf{F}_n^{\text{diff}} = D_n \nabla n, \quad \mathbf{F}_p^{\text{diff}} = D_p \nabla p \tag{2.2.34}$$

The diffusion current densities are derived by multiplying the diffusion fluxes in Eq.2.2.34 by the elementary charge per particle, which is $-q$ for electrons and $+q$ for holes:

$$\mathbf{J}_n^{\text{diff}} = qD_n \nabla n, \quad \mathbf{J}_p^{\text{diff}} = -qD_p \nabla p \tag{2.2.35}$$

The signs in Eq.2.2.35 are choosen such that the diffusion coefficients D_n and D_p are positive.

The electric field driven drift current densities are defined as the products of the elementary charge per particle, the corresponding carrier concentration, and the average electron and hole drift velocities v_n^d and v_p^d, respectively. Thus, the drift current densities are defined as:

$$\mathbf{J}_n^{\text{drift}} = qnv_n^d, \quad \mathbf{J}_p^{\text{drift}} = qpv_p^d \tag{2.2.36}$$

The drift directions of the carriers are assumed to be parallel to the electric field. The drift of holes has the same orientation as the electric field, while the drift of electrons has opposite orientation. Furthermore, the drift velocities are assumed to be proportional to the electric field at moderate electric field strengths [Sze *et al.*]. Thus, the drift velocities for electrons and holes are defined as:

$$v_n^d = -\mu_n \mathbf{E}, \quad v_p^d = \mu_p \mathbf{E}, \tag{2.2.37}$$

where the positive coefficients μ_n and μ_p are the electron and hole mobility, respectively. Thus, inserting Eq.2.2.37 into Eq.2.2.36 gives the drift current density expressions for electrons and holes:

$$\mathbf{J}_n^{\text{drift}} = -q\mu_n n\mathbf{E}, \quad \mathbf{J}_p^{\text{drift}} = q\mu_p p\mathbf{E} \tag{2.2.38}$$

Inserting Eq.2.2.35 and Eq.2.2.38 into Eq.2.2.33 gives the current density equations for electrons and holes:

$$\mathbf{J}_n = q\mu_n n\mathbf{E} + qD_n \nabla n, \quad \mathbf{x} \in \Omega, \quad \mathbf{J}_p = q\mu_p p\mathbf{E} - qD_p \nabla p, \quad \mathbf{x} \in \Omega \tag{2.2.39}$$

The standard practice is to relate the diffusion coefficients D_n and D_p to the mobilities μ_n and μ_p through Einstein's relations:

$$D_n = \frac{k_B \theta_n}{q} \mu_n, \quad D_p = \frac{k_B \theta_p}{q} \mu_p, \tag{2.2.40}$$

where θ_n and θ_p are the carrier lattice temperatures and k_B is Boltzmann's constant, which has a numerical value of $1.3806622 \times 10^{-23}$ J $\cdot$ K^{-1}. Here, the Joule unit J is defined as V $\cdot$ A $\cdot$ s and K stands for kelvin, which is the base unit for the lattice temperatures. A rigorous derivation of the current relations are found in references [Selberherr] and [Selberherr *et al.*].

Drift-Diffusion Model

The following assumptions are made to reach a trade-off between modeling accuracy and simplicity in the isothermal dirft diffusion equations [Markowich]:

- The only sources of current flow are electric field driven convection and diffusion of particle ensembles.
- The diffusion coefficients are defined by Einstein's reations Eq.2.2.40.
- The magnetic inductions vector $\mathbf{B}$ is independent of time. Thus, the electric field in Eq.2.2.19 is recast as:

$$\mathbf{E} = -\nabla\psi. \tag{2.2.41}$$

Isothermal Model

If the assumptions introduced *above* hold and the device temperature is assumed to be an externally defined positive constant, i.e., $\theta \geqq 0$, the isothermal drift-diffusion model is defined as:

$$-\epsilon\Delta\psi = q\left(p - n + N_D^+ - N_A^-\right), \quad \mathbf{x} \in \Omega \quad \text{(Poisson's Equation)} \tag{2.2.42}$$

$$q\frac{\partial n}{\partial t} = \nabla \cdot \mathbf{J}_n - qR, \quad \mathbf{x} \in \Omega \quad \text{(Electron Continuity Equation)} \tag{2.2.43}$$

$$q\frac{\partial p}{\partial t} = -\nabla \cdot \mathbf{J}_p - qR, \quad \mathbf{x} \in \Omega \quad \text{(Hole Continuity Equation)} \tag{2.2.44}$$

$$\mathbf{J}_n = qn\mu_n\mathbf{E}_n + qD_n\nabla n, \quad \mathbf{x} \in \Omega \quad \text{(Electron Transport Equation)} \tag{2.2.45}$$

$$\mathbf{J}_p = qn\mu_p\mathbf{E}_p - qD_p\nabla p, \quad \mathbf{x} \in \Omega \quad \text{(Hole Transport Equation)} \tag{2.2.46}$$

where $\mathbf{E}_n$ and $\mathbf{E}_p$ are the effective electron and hole densities. For metal-oxide-semiconductor, Laplace's equation holds in the oxide:

$$\Delta\psi = 0, \quad \mathbf{x} \in \Phi, \quad t > 0 \tag{2.2.47}$$

The steady state equations are derived from Eq.2.2.42-Eq.2.2.46 by setting

$$\frac{\partial n}{\partial t} = \frac{\partial p}{\partial t} = 0 \tag{2.2.48}$$

Steady state solutions can be interpretated as limits of solutions to the transient problem with similar boundary conditions and arbitrary initial data. Thus, the main objective of stationary (steady state) simulations is to investigate the performance of the semiconductor device after being active for a large-time.

Non-isothermal Model

With the continuous decrease of semiconductor device dimensions, non-isothermal device simulations become important when designing semiconductor devices. The minimization of devices leads to an increase of the dissipated power per volume ratio, which causes a catastrophic local rise of heat. Therefore, non-isothermal simulations are important in determining the thermally stable operating points. The non-isothermal drift-diffusion model solves the Van Roosbroeck equations together with the lattice heat equation to predict current induced self-heating in the device. The non-isothermal drift-diffusion model is defined as:

$$-\epsilon\Delta\psi = q\left(p - n + N_D^+ - N_A^-\right), \quad \mathbf{x} \in \Omega \quad \text{(Poisson's Equation)} \tag{2.2.49}$$

$$q\frac{\partial n}{\partial t} = \nabla \cdot \mathbf{J}_n - qR, \quad \mathbf{x} \in \Omega \quad \text{(Electron Continuity Equation)} \tag{2.2.50}$$

$$q\frac{\partial p}{\partial t} = -\nabla \cdot \mathbf{J}_p - qR, \quad \mathbf{x} \in \Omega \quad \text{(Hole Continuity Equation)} \tag{2.2.51}$$

$$\mathbf{J}_n = qn\mu_n\mathbf{E}_n + qD_n\nabla n + n\mu_n k_B\nabla\theta \quad \mathbf{x}\in\Omega \quad \text{(Electron Transport Equation)} \tag{2.2.52}$$

$$\mathbf{J}_p = qp\mu_p\mathbf{E}_p - qD_p\nabla p - p\mu_p k_B\nabla\theta \quad \mathbf{x}\in\Omega \quad \text{(Hole Transport Equation)} \tag{2.2.53}$$

$$c_v\frac{\partial\theta}{\partial t} - \nabla\cdot(k\nabla\theta) = H, \quad \mathbf{x}\in\Lambda \quad \text{(Lattice Heat Equation)} \tag{2.2.54}$$

where $c_v = \rho c_p$ is the lattice volumetric heat capacity (at constant volume in the case of gas), ρ is the material density, c_p is the specific heat capacity (at constant pressure in the case of gas), k is the lattice thermal conductivity, and H is the heat generated per unit time per unit volume at position $\mathbf{x}$, i.e., heat generation rate. For metal-oxide-semiconductor devices, Eq.2.2.47 (Laplace equation) holds in the oxide. For steady state applications, the time derivatives from Eq.2.2.49-Eq.2.2.54 are ignored.

The heat generation rate is decomposed into a termally-induced heat generation rate term H_θ and an electrically-induced heat generation rate term H_ψ. The electrically-induced heat generation rate term is defined as:

$$H_\psi = \mathbf{J}_n\cdot\mathbf{E}_n + \mathbf{J}_p\cdot\mathbf{E}_p + R\left(E_G + 3k_B\theta\right). \tag{2.2.55}$$

The band gap energy E_G in Eq.2.2.55 is defined as:

$$E_G = E_C - E_V, \tag{2.2.56}$$

where E_C and E_V are the conduction and valence bands. The mathematical form of the effective carrier densities will depend on the type of semiconductor, i.e., *non-degenerate* versus *degenerate*.

Non-Degenerate Case

The electron and hole current densities under isothermal conditions are derived from the Boltzmann transport equations [Marshak]:

$$\mathbf{J}_n = qn\mu_n\mathbf{E}_{f_n}, \quad \mathbf{E}_{f_n} = \nabla E_{f_n} \tag{2.2.57}$$

$$\mathbf{J}_p = qp\mu_p\mathbf{E}_{f_p}, \quad \mathbf{E}_{f_p} = \nabla E_{f_p} \tag{2.2.58}$$

where E_{f_n} and E_{f_p} are the quasi-Fermi levels for electrons and holes, respectively. The expressions defining the relationship between the quasi-Fermi levels and the carrier concentrations are defined as:

$$n = N_C\mathcal{F}(\eta_n), \quad \eta_n = \frac{E_{fn} - E_C}{k_B\theta} \tag{2.2.59}$$

$$p = N_V\mathcal{F}(\eta_p), \quad \eta_p = \frac{E_V - E_{fp}}{k_B\theta}, \tag{2.2.60}$$

where N_C and N_V are the effective densities of states for electron and holes, respectively. E_C and E_V are the energies of the conduction and valence band, respectively. E_{fn} and E_{fp} are the quasi-Fermi energy levels for electrons and holes, respectively. In the non-degenerate case, the relationship between the quasi-Fermi energies and the carrier concentrations is defined by the Maxwell-Boltzmann form:

$$n = N_C\mathcal{F}\left(\eta_n\right) = n_i\exp\left(\frac{E_{fn} - E_i}{k_B\theta}\right) \tag{2.2.61}$$

$$p = N_V\mathcal{F}\left(\eta_p\right) = n_i\exp\left(\frac{E_i - E_{fp}}{k_B\theta}\right), \tag{2.2.62}$$

where n_i is the intrinsic charge carrier density. The intrinsic Fermi level E_i is defined as:

$$E_i = E_0 - \chi - q\psi - \frac{E_G}{2} - \frac{k_B\theta}{2}\ln\left(\frac{N_C}{N_V}\right), \tag{2.2.63}$$

where ψ is the electrostatic potential, $E_G = E_C - E_V$ is the band gap energy, χ is the electron affinity, and E_0 is the reference energy. The quasi-Fermi energy describes the energy level which represents the probability of electron

occupation within a specific energy band (conduction or valence) when a material is not in thermal equilibrium. The quasi-Fermi energy levels for electrons and holes are respectively defined as:

$$E_{fn} = E_i + k_B\theta \ln\left(\frac{n}{n_i}\right) \tag{2.2.64}$$

and

$$E_{fn} = E_i - k_B\theta \ln\left(\frac{p}{n_i}\right). \tag{2.2.65}$$

The drift-diffusion form of the transport equations for the non-degenerate case are derived via the following procedure:

1. Apply the spatial gradient to the carrier concentrations (Eq.2.2.61 and Eq.2.2.62) to derive the the expression for the gradient of the carrier quasi-Fermi energy levels E_{fn} and E_{fp} in terms of the carrier charge densities.
2. Insert the expressions for the gradient of the carrier quasi-Fermi energy level into Eq.2.2.59 and Eq.2.2.60 to derive the drift-diffusion form of the transport equations.

Following the procedure describe above, the drift-diffusion form of the isothermal transport equations for non-degenerancy is defined by Eq.2.2.45 and Eq.2.2.46. Similarly, the drift-diffusion form of the non-isothermal transport equations for non-degenerancy is given by Eq.2.2.52 and Eq.2.2.53. The heat generation rate H in Eq.2.2.54 is computed using Eq.2.2.55. The effective electron and hole densities $\mathbf{E}_n$ and $\mathbf{E}_p$ are replaced with Eq.2.2.41, i.e., the electric field.

Degenerate Case

Degenerate semiconductors experience band structure changes due to the presence of large amount of dopant material, which changes the baseline electron affinity χ and bandgap energy of the material E_G [Schroeder *et al.*]:

$$\Delta\chi = \chi - \chi^{ld} \tag{2.2.66}$$

$$\Delta E_G = E_G^{ld} - E^{ld}, \tag{2.2.67}$$

where the superscript ld denotes low doping. Furthermore, the Pauli principle states that Fermi-Dirac statistics must be used to analyze the physics of a degenerate semiconductor [Pauli]. The carrier current densities under isothermal conditions Eq.2.2.57 and Eq.2.2.58 remain valid[1] when analyzing a degenerate semiconductor. However, the carrier concentrations Eq.2.2.61 and Eq.2.2.62 must be replaced with their Fermi-Dirac statistics counterpart, i.e.,

$$n = N_C\mathcal{F}\left(\eta_n\right) = N_C\mathcal{F}_{1/2}\left(\eta_n\right), \quad \eta_n = \frac{E_{fn} - E_C}{k_B\theta} \tag{2.2.68}$$

$$p = N_V\mathcal{F}\left(\eta_p\right) = N_V\mathcal{F}_{1/2}\left(\eta_p\right), \quad \eta_p = \frac{E_V - E_{fp}}{k_B\theta}, \tag{2.2.69}$$

where the Fermi-Dirac integral of order $1/2$ is defined as:

$$\mathcal{F}_{1/2}(\eta) = \frac{2}{\sqrt{\pi}}\int_0^\infty \frac{\xi^{1/2}}{\exp\left(\xi - \eta\right) + 1} d\xi. \tag{2.2.70}$$

The expressions for the carrier quasi-Fermi energy levels are derived from Eq.2.2.68 and Eq.2.2.69 and are defined as:

$$E_{fn} = E_C + k_B\theta F_{1/2}^{-1}\left(\frac{n}{N_C}\right) \tag{2.2.71}$$

$$E_{fp} = E_V - k_B\theta F_{1/2}^{-1}\left(\frac{p}{N_V}\right), \tag{2.2.72}$$

[1] The carrier mobility decreases as higher concentrations of doping agent are used in a semiconductor.

where $F_{1/2}^{-1}(\cdot)$ denotes the inverse of the Fermi-Dirac integral of order $1/2$. The inverse of the $1/2$ order Fermi-Dirac integral, i.e., given $u = F_{1/2}(\eta)$, η is approximated as follows [Nilsson]:

$$\eta = -\frac{\ln(u)}{u^2-1} + \nu - \frac{\nu}{1+(0.24+1.08\nu)^2}, \quad \text{with} \quad \nu = \left(\frac{3\sqrt{\pi}u}{4}\right)^{2/3} \quad \text{and} \quad u = F_{1/2}(\eta). \tag{2.2.73}$$

The approximation for the inverse of the $1/2$ order Fermi-Dirac integral (Eq.2.2.73) produces an error of less than 0.6 percent over the full range of η.

The carrier density expressions for degenerate semiconductors are defined as:

$$n = n_{ie} \exp\left(\frac{E_{fn} - E_i}{k_B\theta}\right), \tag{2.2.74}$$

$$p = n_{ie} \exp\left(\frac{E_i - E_{fp}}{k_B\theta}\right), \tag{2.2.75}$$

where Eq.2.2.74 and Eq.2.2.75 have a similar form to the carrier density expressions used for *non-degenerate semiconductors*. Eq.2.2.74 and Eq.2.2.75 become equivalent to Eq.2.2.68 and Eq.2.2.69 if n_{ie} and E_i are respectively defined as:

$$E_i = E_0 - \chi - q\psi - \frac{E_G}{2} - \frac{k_B\theta}{2}\ln\left(\frac{N_C\gamma_n}{N_V\gamma_p}\right) \tag{2.2.76}$$

$$n_{ie} = n_{ie}^0\lambda, \tag{2.2.77}$$

where the degeneracy factors γ_n and γ_p are defined as:

$$\gamma_n = \frac{F_{1/2}(\eta_n)}{\exp(\eta_n)} \tag{2.2.78}$$

$$\gamma_p = \frac{F_{1/2}(\eta_p)}{\exp(\eta_p)}. \tag{2.2.79}$$

Recall that η_n and η_p are defined in Eq.2.2.68 and Eq.2.2.69, respectively. The effective intrinsic concentration at equilibrium n_{ie}^0 is defined as:

$$n_{ie}^0 = \sqrt{N_C N_V}\sqrt{F_{1/2}(\eta_n^0)F_{1/2}(\eta_p^0)}, \tag{2.2.80}$$

where the superscript zero on a quantity indicates its equilibrium value. The parameter λ in Eq.2.2.77 is defined as:

$$\lambda = \sqrt{\frac{F_{1/2}(\eta_n)F_{1/2}(\eta_p)}{F_{1/2}(\eta_n^0)F_{1/2}(\eta_p^0)}}\exp\left(\frac{E_{fp} - E_{fn}}{2k_B\theta}\right). \tag{2.2.81}$$

Separating the equilibrium intrinsic concentration n_{ie}^0 and the λ factor that accounts for non-equilibrium from Eq.2.2.77 gives:

$$n_{ie}^0 = n_i \exp\left(\frac{\Delta G^0}{2k_BT}\right), \tag{2.2.82}$$

where the bandgap narrowing ΔG^0 parameter in equilibrium is a known function of the local doping density [Klaassen *et al.*].

The next step is to derive the carrier current densities for a degenerate semiconductor as a function of n, p, and ψ. In contrast to non-degenerate semiconductors, the derivation of the carrier current densities for a degenerate semiconductor is more involved since n_{ie} is not longer a material constant, but a function of the carrier quasi-Fermi potentials and

the band edges. The derivation of $\mathbf{J}_n$ and $\mathbf{J}_p$ begins with taking the gradient of the effective intrinsic concentration with respect to the device configuration, which gives:

$$\nabla n_{ie} = \lambda \nabla n_{ie}^0 + n_{ie}^0 \nabla \lambda. \tag{2.2.83}$$

Eq.2.2.83 is recast as:

$$\nabla n_{ie} = \lambda \nabla n_{ie}^0 + n_{ie}^0 \lambda \nabla \left(\ln \left(\lambda \right) \right). \tag{2.2.84}$$

using the following property: $\nabla x = x \nabla \ln \left(x \right)$ [Schroeder *et al.*]. Taking the gradient of Eq.2.2.82 and using Eq.2.2.77 and Eq.2.2.84 gives:

$$\nabla n_{ie}^0 = \frac{1}{2 k_B \theta} n_{ie}^0 \nabla \left(\Delta G^0 \right). \tag{2.2.85}$$

Finally, with the help of Eq.2.2.85, the gradient of the carrier quasi-Fermi levels are derived by taking the gradient of Eq.2.2.74 and Eq.2.2.75 and solving for the respective gradient of the carrier quasi-Fermi levels:

$$\nabla E_{fn} = k_B \theta \left[\frac{\nabla n}{n} - \nabla \ln \left(\frac{n_{ie}}{n_{ie}^0} \right) \right] - \frac{1}{2} \nabla \left(\Delta G^0 \right) + \nabla E_i \tag{2.2.86}$$

$$\nabla E_{fp} = k_B \theta \left[-\frac{\nabla p}{p} + \nabla \ln \left(\frac{n_{ie}}{n_{ie}^0} \right) \right] + \frac{1}{2} \nabla \left(\Delta G^0 \right) + \nabla E_i. \tag{2.2.87}$$

Inserting Eq.2.2.86 and Eq.2.2.87 into Eq.2.2.57 and Eq.2.2.58 gives the *isothermal transport equations* for degeneracy:

$$\mathbf{J}_n = -qn\mu_n \nabla \psi_n^* + k_B \theta \mu_n \nabla n \tag{2.2.88}$$

$$\mathbf{J}_p = -qp\mu_p \nabla \psi_p^* - k_B \theta \mu_p \nabla p, \tag{2.2.89}$$

where the effective carrier electric potentials ψ_n^* and ψ_p^* are respectively defined as [Schroeder *et al.*]:

$$\nabla \psi_n^* = \nabla \left\{ \frac{\Delta G^0}{2q} + \frac{k_B \theta}{q} \ln \left(\frac{n_{ie}}{n_{ie}^0} \right) + \frac{1}{q} \left[\chi + q\psi + \frac{E_G}{2} + \frac{k_B \theta}{2} \ln \left(\frac{N_C \gamma_n}{N_V \gamma_p} \right) \right] \right\} \tag{2.2.90}$$

$$\nabla \psi_p^* = -\nabla \left\{ \frac{\Delta G^0}{2q} + \frac{k_B \theta}{q} \ln \left(\frac{n_{ie}}{n_{ie}^0} \right) - \frac{1}{q} \left[\chi + q\psi + \frac{E_G}{2} + \frac{k_B \theta}{2} \ln \left(\frac{N_C \gamma_n}{N_V \gamma_p} \right) \right] \right\}. \tag{2.2.91}$$

In the case of the *non-isothermal drift-diffusion model*, the transport equations for degeneracy are defined as:

$$\mathbf{J}_n = -qn\mu_n \nabla \psi_n^* + k_B \theta \mu_n \nabla n + n k_B \mu_n \nabla \theta \tag{2.2.92}$$

$$\mathbf{J}_p = -qp\mu_p \nabla \psi_p^* - k_B \theta \mu_p \nabla p - p k_B \mu_p \nabla \theta, \tag{2.2.93}$$

where ψ_n^* and ψ_p^* are defined by Eq.2.2.90 and Eq.2.2.91, respectively. In addition, the electrically-induced heat generation rate is defined as:

$$H_\psi = \mathbf{J}_n \cdot \nabla \psi_n^* + \mathbf{J}_p \cdot \nabla \psi_p^* + R \left(E_G + 3 k_B \theta \right), \tag{2.2.94}$$

where the electric field $\mathbf{E}$ is replaced with the effective carrier potentials.

If homogeneous semiconductor materials are assumed, it is standard to assume a symmetric partition of the bandgap narrowing on both the conduction and valence bands [Baccarani *et al.*]. Therefore, the following relationship between the change in the electron affinity and the bandgap can be defined:

$$\Delta \chi = \frac{1}{2} \Delta E_G \tag{2.2.95}$$

If Eq.2.2.95, Eq.2.2.66, and Eq.2.2.67 are inserted into Eq.2.2.90 and Eq.2.2.91, the effective carrier potentials are now defined as [Schroeder *et al.*]:

$$\nabla\psi_n^* = \nabla\left[\psi + \frac{\Delta G^0}{2q} + U_\theta \ln\left(\frac{n_{ie}}{n_{ie}^0}\right) + \frac{U_\theta}{2}\ln\left(\frac{\gamma_n}{\gamma_p}\right) + \frac{U_\theta}{2}\ln\left(\frac{N_C}{N_V}\right)\right] \tag{2.2.96}$$

$$\nabla\psi_p^* = \nabla\left[\psi - \frac{\Delta G^0}{2q} - U_\theta \ln\left(\frac{n_{ie}}{n_{ie}^0}\right) + \frac{U_\theta}{2}\ln\left(\frac{\gamma_n}{\gamma_p}\right) + \frac{U_\theta}{2}\ln\left(\frac{N_C}{N_V}\right)\right] \tag{2.2.97}$$

The carrier effective potnetials can be further simplified by neglecting the bias dependence of n_{ie}, i.e.,

$$n_{ie} = n_{ie}^0. \tag{2.2.98}$$

This assumption yields the following set of carrier effective potentials [Schroeder *et al.*]:

$$\nabla\psi_n^* = \nabla\psi + \frac{1}{2q}\nabla\left(\Delta G^0\right) \tag{2.2.99}$$

$$\nabla\psi_p^* = \nabla\psi - \frac{1}{2q}\nabla\left(\Delta G^0\right). \tag{2.2.100}$$

Thus, only the effective bandgap narrowing term impacts the degenerate carrier transport models.

Recombination-Generation Rate

Recombination occurs when a conduction electron becomes a valence electron and neutralises a hole. Generation occurs when a valence electron becomes a conduction electron and leaves a hole. Generation requires energy and recombination sets energy free [Markowich]. The recombination-generation rate R equals zero, i.e., $R \equiv 0$, if the semiconductor is in thermal equilibrium. Recombination dominates when excess carriers are generated and generation dominates when carriers are removed.

Recombination Models

Shockley-Read-Hall

The Shockley-Read-Hall (SRH) model describes a two-step non-radiative recombination process where conduction electrons can relax to the defect level and then relax to the valence band, annihilating a hole in the process [Hall], [Shockley and Read Jr]. Mathematically, the SRH recombination term is defined as:

$$R_{SRH} = \frac{np - n_0 p_0}{\tau_p^l\left(n + \sqrt{n_0 p_0}\right) + \tau_n^l\left(p + \sqrt{n_0 p_0}\right)}, \tag{2.2.101}$$

where τ_n^l and τ_p^l are the electron and hole lifetimes, respectively. The carrier lifetimes can depend on the dopant concentrations. In this case, the carrier lifetime is defined as:

$$\tau = \frac{\tau_0}{1 + \frac{N_D^+ + N_A^-}{N_{srh}}}, \tag{2.2.102}$$

where N_{srh} is a material dependent parameter and N_D and N_A are the respective donor and acceptor concentrations. The equilibrium electron and hole densities are n_0 and p_0, respectively.

Auger

The Auger model describes a non-radiative recombination process where an electron and a hole recombine, but rather than emitting the energy as heat or as a photon, the energy is given to a third carrier, an electron in the conduction band. The third carrier proceeds to thermalize back into the conduction band edge [Auger]. Mathematically, the Auger recombination model is defined as:

$$R_A = \left(C_n n + C_p p\right)\left(np - n_0 p_0\right), \tag{2.2.103}$$

where C_n and C_p are the electron and hole Auger recombination coefficient, respectively. Only constant Auger recombination coefficients are currently supported. The default numerical values are shown in Table 2.2.1. The user is strongly recommended to specify the proper Auger recombination coefficient values when using Eq.2.2.103. The equilibrium electron and hole densities are n_0 and p_0, respectively.

Table 2.2.1: Default numerical values for the Auger recombination coefficients.

Symbol	Numerical Value	Material
C_n	2.8×10^{-31} cm$^6 \cdot$ s^{-1}	Si
C_p	9.9×10^{-32} cm$^6 \cdot$ s^{-1}	Si
C_n	1.0×10^{-30} cm$^6 \cdot$ s^{-1}	GaAs
C_p	1.0×10^{-30} cm$^6 \cdot$ s^{-1}	GaAs

Surface

The surface model describes a non-radiative recombination process where electrons and holes recombine near the surface of a semiconductor device. For the purpose of modeling the surface recombination process, a formula structurally equivalent to the SRH recombination expression is assumed Eq.2.2.101. Mathematically, the model is defined by [Selberherr]:

$$R_{SURF} = \frac{np - n_0 p_0}{s_p^{-1}(n + \sqrt{n_0 p_0}) + s_n^{-1}(p + \sqrt{n_0 p_0})} \delta_{\Gamma_{\text{gate}}}(\mathbf{x}), \tag{2.2.104}$$

where $\delta_{\Gamma_{\text{gate}}}(\mathbf{x})$ is the Dirac distribution concentrated on a Gate contact where surface recombination takes place. The surface recombination velocities for electrons and holes are given by s_n and s_p, respectively.

Boundary Conditions

The boundary conditions of a semiconductor device can be split into two disjoint parts:

$$\Gamma_\Lambda = \Gamma_\Lambda^P \cup \Gamma_\Lambda^A, \quad \Gamma_\Lambda^P \cap \Gamma_\Lambda^A = \{\}. \tag{2.2.105}$$

The real physical boundary Γ_Λ^P usually consists of insulating segments and metal contacts. The artificial boundary Γ_Λ^A is introduced to separate a device from adjacent devices. The device boundaries can be further separated into semiconductor $\Gamma_\Omega = \Gamma_\Omega^P \cup \Gamma_\Omega^A$ and oxide $\Gamma_\Phi = \Gamma_\Phi^P \cup \Gamma_\Phi^A$ boundaries. Thus, $\Gamma_\Lambda = \Gamma_\Omega \cup \Gamma_\Phi = \Gamma_\Omega^P \cup \Gamma_\Omega^A \cup \Gamma_\Phi^P \cup \Gamma_\Phi^A$. Figure Fig. 2.2.1 shows the cross section of a metal-oxide-semiconductor device. The bulk, drain, source, and gate contact boundaries are represented with line segments $\overline{HG}$, $\overline{EF}$, $\overline{AB}$, and $\overline{CD}$, respectively. These collection of line segments represent the physical boundaries. All other boundary line segments are artificial boundaries. Artificial boundaries must not substantially perturb the model [Markowich].

Artificial Boundary Conditions

A standard practice is to assume vanishing outward electric field on the artificial device boundary Γ_Λ^A and vanishing outward current density on the artificial semiconductor boundary Γ_Ω^A, i.e.,

$$\mathbf{E} \cdot \mathbf{n}|_{\Gamma_\Omega^A} = \mathbf{E} \cdot \mathbf{v}|_{\Gamma_\Phi^A} = \mathbf{J}_n \cdot \mathbf{n}|_{\Gamma_\Omega^A} = \mathbf{J}_p \cdot \mathbf{v}|_{\Gamma_\Phi^A} = 0, \tag{2.2.106}$$

where $\mathbf{n}$ is the outward unit normal vector of the semiconductor boundary Γ_Ω and $\mathbf{v}$ is the outward unit normal vector of the oxide boundary Γ_Φ.

Physical Boundary Conditions

The physical semiconductor boundary Γ_Ω^P is generally split into a finite number of contact segments, insulating segments, and semiconductor-oxide interfaces in the case of metal -oxide-semiconductor devices.

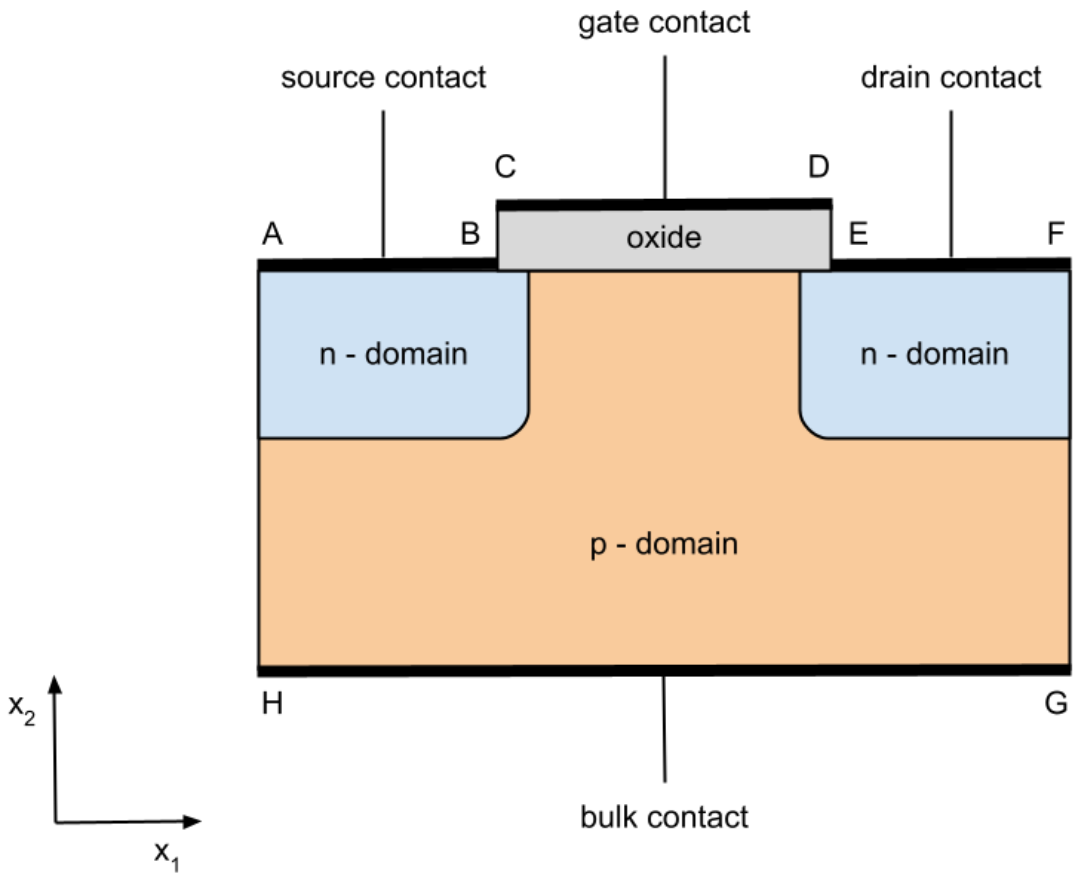

Fig. 2.2.1: Cross section of a metal-oxide-semiconductor device.

Ohmic Contact

Ohmic contact boundary conditions are derived assuming charge neutrality, thermal equilibrium, and dopant ionization. Furthermore, their derivation depend on the carrier statistics choosen to describe the distribution of electrons and holes in a semiconductor device. By imposing charge neutrality and thermal equilibrium conditions, the following relationships are assumed to hold at Ohmic contacts:

$$n_0 p_0 = n_i^2 \tag{2.2.107}$$

$$(n_0 - p_0 - C) = 0 \tag{2.2.108}$$

Dirichlet boundary conditions for the carrier densities and contact potential are derived from Eq.2.2.107 and Eq.2.2.108. Assuming fully ionized dopants and Maxwell-Boltzmann statistics, the Ohmic Dirichlet boundary conditions for n-type semiconductors are defined as:

$$\begin{aligned} n_0 &= \frac{C}{2} + \sqrt{\left(\frac{C}{2}\right)^2 + n_i^2} \\ p_0 &= \frac{n_i^2}{n_0} \\ \psi &= U_\theta \ln(y) + \frac{1}{q}(E_0 - \chi) + \psi_a, \\ y &= \frac{C}{2N_C} + \sqrt{\left(\frac{C}{2N_C}\right)^2 + \frac{N_V}{N_C}\exp\left(-\frac{E_G}{k_B\theta}\right)} \end{aligned} \tag{2.2.109}$$

and for a p-type semiconductors:

$$\begin{aligned} p_0 &= -\frac{C}{2} + \sqrt{\left(\frac{C}{2}\right)^2 + n_i^2} \\ n_0 &= \frac{n_i^2}{p_0} \\ \psi &= -U_\theta \ln(y) + \frac{1}{q}(E_0 - \chi - E_G) + \psi_a \\ y &= -\frac{C}{2N_V} + \sqrt{\left(\frac{C}{2N_V}\right)^2 + \frac{N_C}{N_V}\exp\left(-\frac{E_G}{k_B\theta}\right)} \end{aligned} \tag{2.2.110}$$

The applied potential at an Ohmic contact is represented with ψ_a. E_0 is the Fermi energy of the reference material. E_G is the bandgap energy. N_C is the effective density of states in the conduction band. N_V is the effective density of states in the valence band. The electron affinity in eV is denoted with χ.

For Fermi-Dirac statistics, the thermal equilibrium condition in Eq.2.2.107 is redefined as:

$$n_0 p_0 = \gamma_n \gamma_p n_i^2, \tag{2.2.111}$$

where γ_n and γ_p are the electron and hole degeneracy factors, respectively. If the dopants are fully ionized, the carrier densities and contact potential for n-type semiconductors are given by:

$$\begin{aligned} n_0 &= C \\ p_0 &= N_V \exp\left(-\mathcal{F}_{1/2}^{-1}\left(\frac{n_0}{N_C}\right) - \frac{E_G}{k_B\theta}\right) \\ \psi &= \frac{1}{q}(E_0 - \chi) + \frac{k_B\theta}{q}\mathcal{F}_{1/2}^{-1}\left(\frac{n_0}{N_C}\right) + \psi_a, \end{aligned} \tag{2.2.112}$$

and for p-type semiconductors:

$$\begin{aligned} p_0 &= C \\ n_0 &= N_C \exp\left(-\mathcal{F}_{1/2}^{-1}\left(\frac{p_0}{N_V}\right) - \frac{E_G}{k_B\theta}\right) \\ \psi &= \frac{1}{q}\left(E_0 - \chi - E_G\right) - \frac{k_B\theta}{q}\mathcal{F}_{1/2}^{-1}\left(\frac{p_0}{N_V}\right) + \psi_a. \end{aligned} \tag{2.2.113}$$

The mathematical form of the Fermi-Dirac integral of order $1/2$ is defined by Eq.2.2.70. The explicit evaluation of Eq.2.2.70 is obtained by evaluating the polylogarithm function [Lewin] or via a series representation of the polylogarithm function as described in [Kim *et al.*]. Since the series representation involves summations of infinite series; in practice, the polylogarithm function is evaluated using an approximation or through numerical integration [Press]. The approximation presented in [Bednarczyk and Bednarczyk] is used in the software to evaluate $\mathcal{F}_{1/2}$ due to its simplicity and accuracy[2]. Mathematically, the approximation is defined as:

$$\begin{aligned} \mathcal{F}_{1/2}(\eta) &\approx \left(\exp\left(-\eta\right) + \frac{3\sqrt{\pi}}{4}\nu^{-3/8}\right)^{-1}, \\ \nu &= \eta^4 + 50 + 33.6\eta\left(1 - 0.68\exp\left(-0.17\left(\eta+1\right)^2\right)\right) \end{aligned} \tag{2.2.114}$$

Schottky Contact

A Schottky contact is a metal-semiconductor contact with a considerably large metal-semiconductor barrier height. The height of the barrier influences the device performance by generating a thin region of large space charge [Markowich]. The physics of Schottky contacts is not fully understood and the models used in simulations are simplifications of the phenomenon [Sze *et al.*]. Carriers at Schottky boundaries are assumed to follow Maxwell-Boltzmann statistics. Under these assumptions, the Dirichlet boundary conditions for an n-type and p-type semiconductor are defined as [Bethe]:

$$\begin{aligned} q\psi &= E_0 - W_F + q\psi_a \\ \mathbf{J}_n \cdot \mathbf{n}|_S &= \frac{A_n^* \theta^2}{N_C}\left(n - n_0^S\right) \\ \mathbf{J}_n \cdot \mathbf{p}|_S &= -\frac{A_p^* \theta^2}{N_V}\left(p - p_0^S\right), \end{aligned} \tag{2.2.115}$$

where W_F is the metal work function, ψ_a is the externally applied potential at a Schottky contact, and E_0 is the intrinsic Fermi energy level of the reference material in vacuum. A_n^* and A_p^* are the electron and hole Richardson constants, respectively. The electron density at thermal equilibrium n_0^S is defined as:

$$n_0^S = N_C \exp\left(-\frac{q\psi_S}{k_B\theta}\right) \tag{2.2.116}$$

and the hole density at thermal equilibrium p_0^S is given by:

$$p_0^S = N_V \exp\left(\frac{-E_G + q\psi_S}{k_B\theta}\right). \tag{2.2.117}$$

Insulating Boundary

The following assumptions hold at the insulating semiconductor boundaries Γ_Ω^I:

- Interface charges and surface recombination are neglected; and
- The electric field in the insulating layer vanishes.

[2] The approximation for the polylogarithm function in [Bednarczyk and Bednarczyk] gives a relative error of less than 0.4 percent for $\eta \in (-\infty, \infty)$

Thus, Neumann boundary conditions at insulating semiconductor boundaries Γ_Ω^I are defined as:

$$\mathbf{E}\cdot\mathbf{n}|_{\Gamma_\Omega^I} = \mathbf{J}_n\cdot\mathbf{n}|_{\Gamma_\Omega^I} = \mathbf{J}_p\cdot\mathbf{n}|_{\Gamma_\Omega^I} = 0. \tag{2.2.118}$$

The Neumann boundary conditions at insulating oxide boundaries Γ_Φ^I are defined as:

$$\mathbf{E}\cdot\mathbf{v}|_{\Gamma_\Phi^I} = 0, \tag{2.2.119}$$

where $\mathbf{v}$ is the outward unit normal vector of the oxide boundary Γ_Φ.

Semiconductor-Oxide Interface

Interface charges are neglected along the semiconductor-oxide interface (SOI) Γ_Ω^{SOI}, e.g., represented in Fig. 2.2.1 by the line segment $\overline{BE}$. Thus, the potential ψ and the normal component of the electrical displacement $\mathbf{D}$ to the semiconductor-oxide interface are assumed continuous:

$$[\psi]_{\Gamma_\Omega^{SOI}} = 0 \tag{2.2.120}$$

$$[\mathbf{D}\cdot\mathbf{v}]_{\Gamma_\Omega^{SOI}} = 0. \tag{2.2.121}$$

The height of the jump of function f across the boundary Γ_Ω^{SOI} is denoted with $[f]$. Eq.2.2.121 assumes that the absolute permittivity is piecewise constant, i.e.,

$$\epsilon(\mathbf{x}) = \begin{cases}\epsilon_o, & \mathbf{x}\in\Phi\\ \epsilon_s, & \mathbf{x}\in\Omega\end{cases}, \tag{2.2.122}$$

where ϵ_o and ϵ_s are the oxide and semiconductor absolute permittivity, respectively.

The existence of mobile carriers in the oxide is neglected. Thus, $\mathbf{J}_n|_\Phi \equiv \mathbf{J}_p|_\Phi \equiv 0$. Furthermore, surface recombination effects are neglected on the semiconductor-oxide interface Γ_Ω^{SOI}, which gives:

$$\mathbf{J}_n\cdot\mathbf{v}|_{\Gamma_\Omega^{SOI}} = \mathbf{J}_p\cdot\mathbf{v}|_{\Gamma_\Omega^{SOI}} = 0. \tag{2.2.123}$$

Thus, Eq.2.2.123 states that current does not flow through the semiconductor-oxide interface.

Gate Contact

In practice every oxide domain has a metal contact (gate contact). Gate contacts are modeled by Robin boundary conditions for the electric potential ψ and homogeneous Neumann boundary conditions for the carrier densities:

$$\begin{aligned}&\epsilon_s\nabla\psi\cdot\mathbf{n} + \frac{\epsilon_o}{t_o}\left(\psi - \psi_a - \psi_k\right) = Q_{\text{int}}\\ &\mathbf{J}_n\cdot\mathbf{n} = \mathbf{J}_n\cdot\mathbf{n} = 0\end{aligned}\qquad \mathbf{x}\in\Gamma_G, \tag{2.2.124}$$

where Γ_G denotes the gate contacts, $\mathbf{n}$ is the outward unit normal vector to the contact surface, t_o is the thickness of the oxide, ψ_a is the applied electric potential (voltage) at the gate, ψ_k is the contact electric potential, and Q_{int} is used to account for interface charges. For interfaces to a thick insulator, it is standard to assume a vanishing electric field component perpendicular to the thick interface. Thus, the first term in Eq.2.2.124 reduces to:

$$\epsilon_s\nabla\psi\cdot\mathbf{n} = Q_{int}. \tag{2.2.125}$$

Furthermore, quite often the existence of interface charges are also neglected, i.e., $Q_{int} = 0$.

Initial Guess

The rate of convergence of the Van Roosbroeck equations stronglly depend on the initial guess. The initial guess for dependent variables n, p, and ψ can be estimated for each material region/block. For *isothermal simulations*, the dependent variables for an n-type semiconductor block are initialized as follows:

$$y = \frac{C}{2N_C} + \sqrt{\left(\frac{C}{2N_C}\right)^2 + \frac{N_V}{N_C}\exp\left(-\frac{E_G}{k_B\theta}\right)} \tag{2.2.126}$$

$$\psi = \frac{E_0}{q} - \frac{\chi}{q} + U_\theta \ln(y) \tag{2.2.127}$$

$$n = N_C \exp\left(-\frac{E_C}{k_B\theta}\right) \tag{2.2.128}$$

$$p = N_V \exp\left(\frac{E_V}{k_B\theta}\right) \tag{2.2.129}$$

and for p-type semiconductor block:

$$y = -\frac{C}{2N_V} + \sqrt{\left(\frac{C}{2N_V}\right)^2 + \frac{N_C}{N_V}\exp\left(-\frac{E_G}{k_B\theta}\right)} \tag{2.2.130}$$

$$\psi = \frac{E_0}{q} - \frac{\chi}{q} + \frac{E_G}{q} - U_\theta \ln(y) \tag{2.2.131}$$

$$n = N_C \exp\left(-\frac{E_C}{k_B\theta}\right) \tag{2.2.132}$$

$$p = N_V \exp\left(\frac{E_V}{k_B\theta}\right), \tag{2.2.133}$$

where the doping profile C is defined by Eq.2.2.26. For *non-isothermal simulations*, the initial guess for an n-type semiconductor block is computed as follows:

$$T(\theta) = \frac{\chi}{q} + \frac{E_G}{2q} + \frac{k_B\theta}{2q}\ln\left(\frac{N_C}{N_V}\right) \tag{2.2.134}$$

$$y = \frac{C}{2N_C} + \sqrt{\left(\frac{C}{2N_C}\right)^2 + \frac{N_V}{N_C}\exp\left(-\frac{E_G}{k_B\theta}\right)} \tag{2.2.135}$$

$$\psi = T(\theta) - \frac{\chi}{q} + \frac{k_B\theta}{q}\ln(y) \tag{2.2.136}$$

$$n = N_C \exp\left(-\frac{E_C}{k_B\theta}\right) \tag{2.2.137}$$

$$p = N_V \exp\left(\frac{E_V}{k_B\theta}\right) \tag{2.2.138}$$

and for a p-type semiconductor block:

$$T(\theta) = \frac{\chi}{q} + \frac{E_G}{2q} + \frac{k_B\theta}{2q}\ln\left(\frac{N_C}{N_V}\right) \tag{2.2.139}$$

$$y = -\frac{C}{2N_V} + \sqrt{\left(\frac{C}{2N_V}\right)^2 + \frac{N_C}{N_V}\exp\left(-\frac{E_G}{k_B\theta}\right)} \tag{2.2.140}$$

$$\psi = T(\theta) - \frac{\chi}{q} + \frac{E_G}{q} - \frac{k_B\theta}{q}\ln(y) \tag{2.2.141}$$

$$n = N_C \exp\left(-\frac{E_C}{k_B\theta}\right) \tag{2.2.142}$$

$$p = N_V \exp\left(\frac{E_V}{k_B\theta}\right) \tag{2.2.143}$$

Constructing an initial guess for a drift-diffusion simulation requires two steps. First, Eq.2.2.42 must be solved with an appropriate initial guess for the electric potential ψ. The equations used to compute the initial guess for the electric potential will depend on the type of semiconductor block and the type of thermodynamic process (isothermal versus non-isothermal). Second, Eq.2.2.43 and Eq.2.2.44 are solved to obtained the initial guess for n and p, respectively. The solution to Eq.2.2.42 serves as the initial guess for the electric potential when computing the initial guess for the charge carrier densities.

Table 2.2.2: Scaling factors and their typical numerical values.

Symbol	Description	Scaling Factor	Numerical Value
x_i	i-th spatial coordinate	x_o [cm]	5.0×10^{-3}
C	doping profile	C_o [cm^{-3}]	10^{17}
D	diffusion coefficient	D_o [$\text{cm}^2 \cdot \text{s}^{-1}$]	36
θ	temperature	θ_o [K]	300
ψ	electric potential	U_θ [V]	0.0259
n	electron concentration	C_o [cm^{-3}]	10^{17}
p	hole concentration	C_o [cm^{-3}]	10^{17}
n_i	intrinsic carrier concentration	C_o [cm^{-3}]	10^{17}
c_v	volumetric heat capacity	c_{v_o} [$\text{J} \cdot \text{cm}^{-3} \cdot \text{K}^{-1}$]	2.3
t	time variable	t_o [s]	x_o^2/D_o
$\mathbf{J}_n$	electron current density	$\mathbf{J}_{n_o}$ [$A \cdot \text{cm}^{-2}$]	$(qD_oC_o)/x_o$
$\mathbf{J}_p$	hole current density	$\mathbf{J}_{p_o}$ [$A \cdot \text{cm}^{-2}$]	$(qD_oC_o)/x_o$
μ_n	electron mobility	μ_{n_o} [$\text{cm}^2 \cdot \text{V}^{-1} \cdot \text{s}^{-1}$]	D_o/U_θ
μ_p	hole mobility	μ_{p_o} [$\text{cm}^2 \cdot \text{V}^{-1} \cdot \text{s}^{-1}$]	D_o/U_θ
R	recombination-generation rate	R_o [$\text{cm}^{-3} \cdot \text{s}^{-1}$]	$(D_oC_o)/x_o^2$
τ_n^l	electron lifetime	$\tau_{n_o}^l$ [s]	x_o^2/D_o
τ_p^l	hole lifetime	$\tau_{p_o}^l$ [s]	x_o^2/D_o
H	heat generation rate	H_o [W/cm^3]	$(c_{v_o}\theta_o)/t_o$
k	thermal conductivity	k_o [$\text{W} \cdot \text{cm}^{-1} \cdot \text{K}^{-1}$]	$(H_ox_o^2)/\theta_o$

Singular Perturbation Scaling

Identifying and applying an appropriate scaling to the dependent variables (ψ, n, p) is standard practice when solving the Van Roosbroeck equations Eq.2.2.42- Eq.2.2.46 due to the different orders of magnitude observed in the dependent variables. The scaling used here is presented in references [Markowich and Ringhofer], [Markowich], [Markowich], [Selberherr] and it is based on the following assumptions:

- A characteristic device length l is chosen such that it is of the same order of magnitude as the diameter of the computational semiconductor domain Ω, i.e.,

$$l = O(\text{diam}(\Omega)). \tag{2.2.144}$$

- All potentials are scaled by the thermal voltage U_θ.
- Carrier concentrations are scaled by a characteristic doping concentration C_0, which is chosen such that the following holds:

$$C_{\max} := \max_{\Omega} |C|, \quad C_0 = O(C_{\max}) \tag{2.2.145}$$

- The carrier mobilities are scaled by a reference mobility μ_0 such that μ_n/μ_0 and μ_p/μ_0 are maximally of the order of magnitude 1.0.

The scaling Eq.2.2.145 facilitates the scaled majority carrier concentrations at Ohmic contacts to be maximally of the order of magnitude 1.0. The scaling factors and their typical numerical values are tabulated in Table 2.2.2 [Markowich].

Isothermal Drift-Diffusion Model

By substituting the scaling factors in Table 2.2.2 into Eq.2.2.42-Eq.2.2.46, the scaled isothermal Van Roosbroeck equations are defined as:

$$-\lambda_{\psi}^{2}\Delta\widehat{\psi} = \widehat{p} - \widehat{n} + \widehat{C}, \quad \widehat{\mathbf{x}} \in \Omega \quad \text{(Poisson's Equation)} \tag{2.2.146}$$

$$\frac{\partial\widehat{n}}{\partial\widehat{t}} = \nabla\cdot\widehat{\mathbf{J}}_{n} - \widehat{R}, \quad \widehat{\mathbf{x}} \in \Omega \quad \text{(Electron Continuity Equation)} \tag{2.2.147}$$

$$\frac{\partial\widehat{p}}{\partial\widehat{t}} = -\nabla\cdot\widehat{\mathbf{J}}_{p} - \widehat{R}, \quad \widehat{\mathbf{x}} \in \Omega \quad \text{(Hole Continuity Equation)} \tag{2.2.148}$$

$$\widehat{\mathbf{J}}_{n} = \widehat{\mu}_{n}\nabla\widehat{n} + \widehat{n}\boldsymbol{\upsilon}_{n}^{eff}, \quad \widehat{\mathbf{x}} \in \Omega \quad \text{(Electron Transport Equation)} \tag{2.2.149}$$

$$\widehat{\mathbf{J}}_{p} = -\widehat{\mu}_{p}\nabla\widehat{p} + \widehat{p}\boldsymbol{\upsilon}_{p}^{eff}, \quad \widehat{\mathbf{x}} \in \Omega \quad \text{(Hole Transport Equation)}, \tag{2.2.150}$$

where the effective carrier velocities in the carrier continutity equations are defined as:

$$\boldsymbol{\upsilon}_{n}^{eff} = \widehat{\mu}_{n}\nabla\widehat{\psi} \tag{2.2.151}$$

$$\boldsymbol{\upsilon}_{p}^{eff} = -\widehat{\mu}_{p}\nabla\widehat{\psi}. \tag{2.2.152}$$

The scaling parameter λ_{ψ} in Eq.2.2.146 is defined as:

$$\lambda_{\psi} = \frac{\lambda_{D}}{l}, \quad \lambda_{D} = \sqrt{\frac{\epsilon_{r}\epsilon_{0}U_{\theta}}{qC_{o}}}. \tag{2.2.153}$$

The parameter λ_{D} is the characteristic Debye length of the device. The Debye length is a measure of how far into the plasma the potential of an electrode or probe is observed [Debye and Hückel]. The hat notation is used in this manuscript to specify a scaled variable. Finally, the time derivatives in Eq.2.2.146-Eq.2.2.150 are ignored for steady state applications.

Non-isothermal Drift-Diffusion Model

The scaled form of the non-isothermal drift-diffusion model is defined as:

$$-\lambda_{\psi}^{2}\Delta\widehat{\psi} = \widehat{p} - \widehat{n} + \widehat{C}, \quad \widehat{\mathbf{x}} \in \Omega \quad \text{(Poisson's Equation)} \tag{2.2.154}$$

$$\frac{\partial\widehat{n}}{\partial\widehat{t}} = \nabla\cdot\widehat{\mathbf{J}}_{n} - \widehat{R}, \quad \widehat{\mathbf{x}} \in \Omega \quad \text{(Electron Continuity Equation)} \tag{2.2.155}$$

$$\frac{\partial\widehat{p}}{\partial\widehat{t}} = -\nabla\cdot\widehat{\mathbf{J}}_{p} - \widehat{R}, \quad \widehat{\mathbf{x}} \in \Omega \quad \text{(Hole Continuity Equation)} \tag{2.2.156}$$

$$\widehat{\mathbf{J}}_{n} = \widehat{\mu}_{n}\nabla\widehat{n} + \widehat{n}\boldsymbol{\upsilon}_{n}^{eff}, \quad \widehat{\mathbf{x}} \in \Omega \quad \text{(Electron Transport Equation)} \tag{2.2.157}$$

$$\widehat{\mathbf{J}}_{p} = -\widehat{\mu}_{p}\nabla\widehat{p} + \widehat{p}\boldsymbol{\upsilon}_{p}^{eff}, \quad \widehat{\mathbf{x}} \in \Omega \quad \text{(Hole Transport Equation)} \tag{2.2.158}$$

$$\widehat{c}_{v}\frac{\partial\widehat{\theta}}{\partial\widehat{t}} - \nabla\cdot\left(\widehat{k}\nabla\widehat{\theta}\right) = \widehat{H}, \quad \widehat{\mathbf{x}} \in \Lambda \quad \text{(Lattice Heat Equation)}. \tag{2.2.159}$$

The carrier effective velocities are defined as:

$$\boldsymbol{\upsilon}_{n}^{eff} = \widehat{\mu}_{n}\nabla\psi + \widehat{\mu}_{n}\nabla\theta \tag{2.2.160}$$

$$\boldsymbol{\upsilon}_{p}^{eff} = -\widehat{\mu}_{p}\nabla\psi - \widehat{\mu}_{p}\nabla\theta \tag{2.2.161}$$

The time derivatives in Eq.2.2.154 - Eq.2.2.159 are ignored for steady state applications.

Boundary Conditions

Clearly, the source terms and boundary conditions presented in sections *Recombination-Generation Rate* and *Boundary Conditions* must be expressed in terms of the scaled variables. For instance, the scaled *Shockley-Read-Hall recombination-generation term* is defined as:

$$R_{SRH} = \frac{\widehat{n}\widehat{p} - \delta^4}{\widehat{\tau}_p^l(\widehat{n} + \delta^2) + \widehat{\tau}_n^l(\widehat{p} + \delta^2)}, \tag{2.2.162}$$

where $\widehat{\tau}_{n,p}^l = \tau_{n,p}^l/\tau_o$, with $\tau_o = x_o^2/D_o$. The scaled intrinsic number δ is defined as:

$$\delta = \sqrt{\frac{n_0 p_0}{C_o}}. \tag{2.2.163}$$

The mathematical expressions for the charge carrier densities n_0 and p_0 differ for *non-degenerate* and *degenerate* semiconductors.

The scaled Ohmic contact boundary conditions for n-type semiconductors are defined as:

$$\begin{aligned}
\widehat{n}_o &= \frac{1}{2}\left(\widehat{C} + \sqrt{\widehat{C}^2 + 4\delta^4}\right), \\
\widehat{p}_o &= \frac{\delta^2}{\widehat{n}_o}, \\
\widehat{\psi}_o &= \ln(y) + \frac{1}{qU_\theta}(E_0 - \chi) + \widehat{\psi}_a, \\
y &= \frac{C}{2N_C} + \sqrt{\left(\frac{C}{2N_C}\right)^2 + \frac{N_V}{N_C}\exp\left(-\frac{E_G}{k_B\theta}\right)},
\end{aligned} \tag{2.2.164}$$

and for p-type semiconductors:

$$\begin{aligned}
\widehat{p}_o &= \frac{1}{2}\left(-\widehat{C} + \sqrt{\widehat{C}^2 + 4\delta^4}\right), \\
\widehat{n}_o &= \frac{\delta^2}{\widehat{p}_o}, \\
\widehat{\psi}_o &= -\ln(y) + \frac{1}{qU_\theta}(E_0 - \chi - E_G) + \widehat{\psi}_a, \\
y &= -\frac{C}{2N_V} + \sqrt{\left(\frac{C}{2N_V}\right)^2 + \frac{N_C}{N_V}\exp\left(-\frac{E_G}{k_B\theta}\right)},
\end{aligned} \tag{2.2.165}$$

where $\widehat{\psi}_a = \psi_a/U_\theta$. Maxwell-Boltzmann statistics were assumed in the derivation of Eq.2.2.164 and Eq.2.2.165. The derivation for Fermi-Dirac statistics follows analogously.

Weak Formulation

Let $H^1(\Omega)$ be the Sobolev space of weakly differentiable functions and $H_D^1(\Omega) = \{w \in H^1(\Omega) | w = 0 \text{ on } \Gamma_D\}$, with Γ_D defined as the Dirichlet boundary. The scaled variational form of the *isothermal drift-diffusion model* is defined as:

Poisson's Equation

$$\begin{aligned}
\widehat{\mathbf{R}}_1(\widehat{\psi}, \widehat{n}, \widehat{p}) = \lambda_\psi^2 \int_\Omega \nabla w \cdot \nabla\widehat{\psi}\, d\Omega - \lambda_\psi^2 \int_\Gamma w(\nabla\widehat{\psi}\cdot\mathbf{n})\, d\Gamma \\
- \int_\Omega w\left(\widehat{p} - \widehat{n} + \widehat{C}\right)\, d\Omega = 0, \quad w \in H^1(\Omega)
\end{aligned} \tag{2.2.166}$$

Electron Continuity Equation

$$\widehat{\mathbf{R}}_2(\widehat{\psi},\widehat{n},\widehat{p}) = \int_\Omega w\frac{\partial \widehat{n}}{\partial \widehat{t}}\,d\Omega + \int_\Omega \nabla w\cdot\widehat{\mathbf{J}}_n\,d\Omega - \int_\Gamma w\left(\widehat{\mathbf{J}}_n\cdot\mathbf{n}\right)\,d\Gamma + \int_\Omega w\widehat{R}\,d\Omega = 0, \quad w\in H^1(\Omega) \tag{2.2.167}$$

Hole Continuity Equation

$$\widehat{\mathbf{R}}_3(\widehat{\psi},\widehat{n},\widehat{p}) = \int_\Omega w\frac{\partial \widehat{p}}{\partial \widehat{t}}\,d\Omega - \int_\Omega \nabla w\cdot\widehat{\mathbf{J}}_p\,d\Omega + \int_\Gamma w\left(\widehat{\mathbf{J}}_p\cdot\mathbf{n}\right)\,d\Gamma + \int_\Omega w\widehat{R}\,d\Omega = 0, \quad w\in H^1(\Omega) \tag{2.2.168}$$

where w denotes the test function. For an isothermal thermodynamic process, the carrier current densities $\mathbf{J}_n$ and $\mathbf{J}_p$ are defined by Eq.2.2.149 and Eq.2.2.150, respectively. The product rule $\nabla(a\mathbf{b}) = \nabla a\cdot\mathbf{b} + a\nabla\cdot\mathbf{b}$, for the product of a scalar a and a vector $\mathbf{b}$, was used in the derivation of the variational form of the drift-diffusion model to reduce the derivative order on an expression in conjunction with the divergence theorem.

For a *non-isothermal thermodynamic process*, the scaled variational form of the drift-diffusion model form follows Eq.2.2.166 - Eq.2.2.168. However, the carrier continutity equations depend on the temperature field θ through the carrier current densities, i.e., Eq.2.2.157 and Eq.2.2.158. Therefore, the lattice heat equation needs to be solved to predict current induced self-heating in the device. The scaled variational form of the lattice heat equation is defined as:

Lattice Heat Equation

$$\widehat{\mathbf{R}}_4(\widehat{\psi},\widehat{n},\widehat{p},\widehat{\theta}) = \int_\Omega w\left(\widehat{c}_v\frac{\partial\widehat{\theta}}{\partial\widehat{t}}\right)\,d\Omega + \int_\Omega \nabla w\cdot\left(\widehat{k}\nabla\widehat{\theta}\right)\,d\Omega - \int_\Gamma w\widehat{q}_0\,d\Gamma - \int_\Omega w\widehat{H}\,d\Omega = 0,\ w\in H^1(\Omega), \tag{2.2.169}$$

For non-degenerate semiconductors, the heat generation rate H is defined by Eq.2.2.55. In the case of degenerate semiconductors, H is defined by Eq.2.2.94.

Stabilization

The backward Euler time integration scheme, i.e., implicit Euler, is used to approximate the time derivate. The backward Euler scheme is unconditionally stable. Therefore, the numerical stability of the discretized drift-diffusion model depends mainly on selecting a stable spatial discretization method. The Poisson and Lattice Heat equations do not need stabilization when discretized with a standard finite element method. However, standard finite element methods are not suited for problems where the behavior of the dependent variable is almost singular [Miller *et al.*], e.g., the charge carrier densities. Therefore, the carrier continutity equations must be discretized using a non-standard finite element method.

The Symmetrized Exponentially Fitted Flux Galerkin (Sym-EFFG) finite element method is applied to avoid numerical pathologies in the carrier continuity equations [Bochev *et al.*]. The Sym-EFFG finite element method adds a stabilization term to the carrier continuity equations to avoid unphysical spurious oscillations in the numerical solution. The Sym-EFFG stabilization term, in the case of the electron continuity equation, is defined as:

$$\begin{aligned} R_{\Theta_n}(\widehat{\psi},\widehat{n}) &= \int_\Omega \Theta(\widehat{n})\cdot\Theta(w)\,d\Omega \\ &= \int_\Omega \left(\sum_{e_\alpha\in E(\Omega)} \vartheta_\alpha\left(\widehat{n}_{\alpha_2}-\widehat{n}_{\alpha_1}\right)\mathbf{N}_\alpha\right)\cdot\left(\sum_{e_\beta\in E(\Omega)}\vartheta_\beta\left(w_{\beta_2}-w_{\beta_1}\right)\mathbf{N}_\beta\right)\,d\Omega, \end{aligned} \tag{2.2.170}$$

where

$$\vartheta_\alpha = \sqrt{D_\alpha P_\alpha\left(\coth(P_\alpha)-\frac{1}{P_\alpha}\right)}, \quad P_\alpha = \frac{h_\alpha v_\alpha^{eff}}{2D_\alpha}. \tag{2.2.171}$$

The parameter $E(\Omega)$ denotes the set of all edges assigned to a finite element. An edge e_α begins at node α_1 and ends at node α_2. Edges are labeled with a multi-index $\alpha = (\alpha_1, \alpha_2)$ comprising the indices of their endpoints, i.e., e_α is an edge with endpoints p_{α_1} and p_{α_2}. The Peclet number P_α is associated with edge e_α, where D_α is the edge diffusion coefficient and υ_α is the edge advective velocity. The edge advective velocity is defined as:

$$\upsilon_\alpha = \|\boldsymbol{\upsilon}_n^{eff}\| \mathrm{v}_\alpha, \quad \mathrm{v}_\alpha = \left(\frac{\boldsymbol{\upsilon}_n^{eff}}{\|\boldsymbol{\upsilon}_n^{eff}\|} \right) \cdot \mathbf{t}_\alpha, \quad \mathbf{t}_\alpha = g_{\alpha,\alpha_1} \frac{(p_{\alpha_1} - p_{\alpha_2})}{\|p_{\alpha_1} - p_{\alpha_2}\|}, \tag{2.2.172}$$

where

$$g_{\alpha,j} = \begin{cases} -1 & \text{if } p_{\alpha_j} \text{ is the first vertex of } e_\alpha \\ 1 & \text{if } p_{\alpha_j} \text{ is the second vertex of } e_\alpha \end{cases} \tag{2.2.173}$$

The parameter h_α denotes the edge length. The electron densities at vertex p_{α_1} and vertex p_{α_2} are given by n_{α_1} and n_{α_2}, respectively. The vector $\mathbf{N}_\alpha$ holds the basis functions for edge e_α. The expression for the effective carrier drift velocities $\boldsymbol{\upsilon}_n^{eff}$ depend on the thermodynamic process. If the thermodynamic process is isothermal, the effective carrier drift velocities are defined by Eq.2.2.151 and Eq.2.2.152. If the thermodynamic process is non-isothermal, the effective carrier drift velocities are defined by Eq.2.2.160 and Eq.2.2.161.The derivation of the Sym-EFFG stabilization term for the hole continuity equation follows analogously.

Adding the Sym-EFFG stabilization term to the *variational form of the carrier continuity equations* gives the stabilized form for the isothermal drift-diffusion model:

$$\begin{aligned} &\mathbf{R}_1(\widehat{\psi}, \widehat{n}, \widehat{p}) = \widehat{\mathbf{R}}_1(\widehat{\psi}, \widehat{n}, \widehat{p}) = 0, \quad w \in H^1(\Omega) \\ &\mathbf{R}_2(\widehat{\psi}, \widehat{n}, \widehat{p}) = \widehat{\mathbf{R}}_2(\widehat{\psi}, \widehat{n}, \widehat{p}) + \mathbf{R}_{\Theta_n^\psi}(\widehat{\psi}, \widehat{n}) = 0, \quad w \in H^1(\Omega) \\ &\mathbf{R}_3(\widehat{\psi}, \widehat{n}, \widehat{p}) = \widehat{\mathbf{R}}_3(\widehat{\psi}, \widehat{n}, \widehat{p}) + \mathbf{R}_{\Theta_p^\psi}(\widehat{\psi}, \widehat{p}) = 0, \quad w \in H^1(\Omega), \end{aligned} \tag{2.2.174}$$

where the Sym-EFFG stabilization term is defined by Eq.2.2.170. The non-isothermal drift-diffusion model is defined as:

$$\begin{aligned} &\mathbf{R}_1(\widehat{\psi}, \widehat{n}, \widehat{p}) = \widehat{\mathbf{R}}_1(\widehat{\psi}, \widehat{n}, \widehat{p}) = 0, \quad w \in H^1(\Omega) \\ &\mathbf{R}_2(\widehat{\psi}, \widehat{n}, \widehat{p}, \widehat{\theta}) = \widehat{\mathbf{R}}_2(\widehat{\psi}, \widehat{n}, \widehat{p}, \widehat{\theta}) + \mathbf{R}_{\Theta_n^\psi}(\widehat{\psi}, \widehat{n}, \widehat{\theta}) = 0, \quad w \in H^1(\Omega) \\ &\mathbf{R}_3(\widehat{\psi}, \widehat{n}, \widehat{p}, \widehat{\theta}) = \widehat{\mathbf{R}}_3(\widehat{\psi}, \widehat{n}, \widehat{p}, \widehat{\theta}) + \mathbf{R}_{\Theta_p^\psi}(\widehat{\psi}, \widehat{p}, \widehat{\theta}) = 0, \quad w \in H^1(\Omega) \\ &\mathbf{R}_4(\widehat{\psi}, \widehat{n}, \widehat{p}, \widehat{\theta}) = \widehat{\mathbf{R}}_4(\widehat{\psi}, \widehat{n}, \widehat{p}, \widehat{\theta}) = 0, \quad w \in H^1(\Lambda). \end{aligned} \tag{2.2.175}$$

In contrast to the Streamline Upwind Petrov Galerkin (SUPG) stabilization method [Brooks and Hughes], the Sym-EFFG stabilization method produces a symmetric stabilization operator. In addition, the Sym-EFFG stabilization method does not rely on problem-specific stabilization parameters, which is the case with SUPG stabilization. For completeness, the SUPG stabilization term is defined for the electron continuity equation:

$$\int_\Omega \tau_n \left(\boldsymbol{\upsilon}_n^{eff} \cdot \nabla n \right) \left(\boldsymbol{\upsilon}_n^{eff} \cdot \nabla w \right) \, d\Omega, \tag{2.2.176}$$

where $\boldsymbol{\upsilon}_n^{eff}$ is the effective electron drift velocity. The stabilization parameter τ_n is defined as:

$$\tau_n = \frac{1}{\boldsymbol{\upsilon}_n^{eff} \boldsymbol{G}_c \boldsymbol{\upsilon}_n^{eff}} \left[\coth(P_n) - \frac{1}{P_n} \right], \quad P_n = \frac{\sqrt{(\boldsymbol{\upsilon}_n^{eff})^T \boldsymbol{G}_c \boldsymbol{\upsilon}_n^{eff}}}{D_n \|\boldsymbol{G}_c\|}, \tag{2.2.177}$$

where $\boldsymbol{G}_c$ is the finite element contravariant tensor, D_n is the electron diffusion coefficient, and P_n is the electron Peclet number (Eq.2.2.173). The derivation of the SUPG stabilization term for the hole continuity equation follows analogously.

If τ_n is used with the Sym-EFFG stabilization method of Eq.2.2.170, Eq.2.2.177 is recovered. However, in addition to the SUPG stabilization parameter, an additional crosswind diffusion term in the direction perpendicular to the dominant

advective/drift velocity direction is derived [Mamaluy *et al.*]. The additional crosswind stabilization discourages unphysical spurious oscillations in the numerical solution when crosswind velocities are dominant. Thus, the Sym-EFFG stabilization method is able to outperform the SUPG stabilization method when crosswind velocities are dominant. However, if the crosswind velocities are small, the Sym-EFFG and SUPG stabilization methods will produce similar stabilization effects [Mamaluy *et al.*].

Solution Method

The most popular algorithms for the iterative treatment of Eq.2.2.174 are the fully coupled Newton's method (Eq.1.2.1) and the decoupled Gummel map. System Eq.2.2.174 can be written in compact form as:

$$\mathbf{R}\left(\mathbf{u}\right) = \mathbf{0}, \tag{2.2.178}$$

where

$$\mathbf{u} := \left[\widehat{\psi}, \widehat{n}, \widehat{p}\right]^T, \qquad \mathbf{R}\left(\mathbf{u}\right) := \begin{bmatrix} \mathbf{R}_1(\mathbf{u}) \\ \mathbf{R}_2(\mathbf{u}) \\ \mathbf{R}_3(\mathbf{u}) \end{bmatrix} \tag{2.2.179}$$

for isothermal thermodynamic processes and

$$\mathbf{u} := \left[\widehat{\psi}, \widehat{n}, \widehat{p}, \widehat{\theta}\right]^T, \qquad \mathbf{R}\left(\mathbf{u}\right) := \begin{bmatrix} \mathbf{R}_1(\mathbf{u}) \\ \mathbf{R}_2(\mathbf{u}) \\ \mathbf{R}_3(\mathbf{u}) \\ \mathbf{R}_4(\mathbf{u}) \end{bmatrix} \tag{2.2.180}$$

for non-isothermal thermodynamic processes.

Fully Coupled Newton's Method

Linearization of the residual $\mathbf{R}\left(\mathbf{u}\right)$ gives the following linear system of equations:

$$\mathbf{J}(\mathbf{u})\delta\mathbf{u} = -\mathbf{R}(\mathbf{u}), \tag{2.2.181}$$

where $\delta\mathbf{u} = [\delta\psi, \delta n, \delta p]^T$ is the perturbation vector and $\mathbf{J}(\mathbf{u})$ is the Jacobian. For an isothermal thermodynamic process, the Jacobian is defined as:

$$\mathbf{J}(\mathbf{u}) := \begin{bmatrix} \mathbf{R}_{1,\psi}(\mathbf{u}) & \mathbf{R}_{1,n}(\mathbf{u}) & \mathbf{R}_{1,p}(\mathbf{u}) \\ \mathbf{R}_{2,\psi}(\mathbf{u}) & \mathbf{R}_{2,n}(\mathbf{u}) & \mathbf{R}_{2,p}(\mathbf{u}) \\ \mathbf{R}_{3,\psi}(\mathbf{u}) & \mathbf{R}_{3,n}(\mathbf{u}) & \mathbf{R}_{3,p}(\mathbf{u}) \end{bmatrix}, \tag{2.2.182}$$

where $\mathbf{u}$ is defined by Eq.2.2.179. In the case of a non-isothermal thermodynamic process, the Jacobian is defined as:

$$\mathbf{J}(\mathbf{u}) := \begin{bmatrix} \mathbf{R}_{1,\psi}(\mathbf{u}) & \mathbf{R}_{1,n}(\mathbf{u}) & \mathbf{R}_{1,p}(\mathbf{u}), & \mathbf{R}_{1,\theta}(\mathbf{u}) \\ \mathbf{R}_{2,\psi}(\mathbf{u}) & \mathbf{R}_{2,n}(\mathbf{u}) & \mathbf{R}_{2,p}(\mathbf{u}), & \mathbf{R}_{2,\theta}(\mathbf{u}) \\ \mathbf{R}_{3,\psi}(\mathbf{u}) & \mathbf{R}_{3,n}(\mathbf{u}) & \mathbf{R}_{3,p}(\mathbf{u}), & \mathbf{R}_{3,\theta}(\mathbf{u}) \\ \mathbf{R}_{4,\psi}(\mathbf{u}) & \mathbf{R}_{4,n}(\mathbf{u}) & \mathbf{R}_{4,p}(\mathbf{u}), & \mathbf{R}_{4,\theta}(\mathbf{u}) \end{bmatrix}, \tag{2.2.183}$$

where $\mathbf{u}$ is defined by Eq.2.2.180.

The subscript (i, j) notation used in Eq.2.2.182 and Eq.2.2.183 specifies the partial derivatives of the $i-th$ residual with respect to the $j-th$ dependent variable. For instance, subscript $(1, p)$ denotes the partial derivatives of residual $\mathbf{R}_1(\mathbf{u})$ with respect to the hole density p. *Newton's method* is used to solve Eq.2.2.181 for $\delta\mathbf{u}^k$ at each iteration $k > 0$ as follows:

$$\begin{aligned} \delta\mathbf{u}^k &= -\mathbf{J}(\mathbf{u}^k)^{-1}\mathbf{R}(\mathbf{u}^k), \\ \mathbf{u}^{k+1} &= \mathbf{u}^k + \delta\mathbf{u}^k \end{aligned} \tag{2.2.184}$$

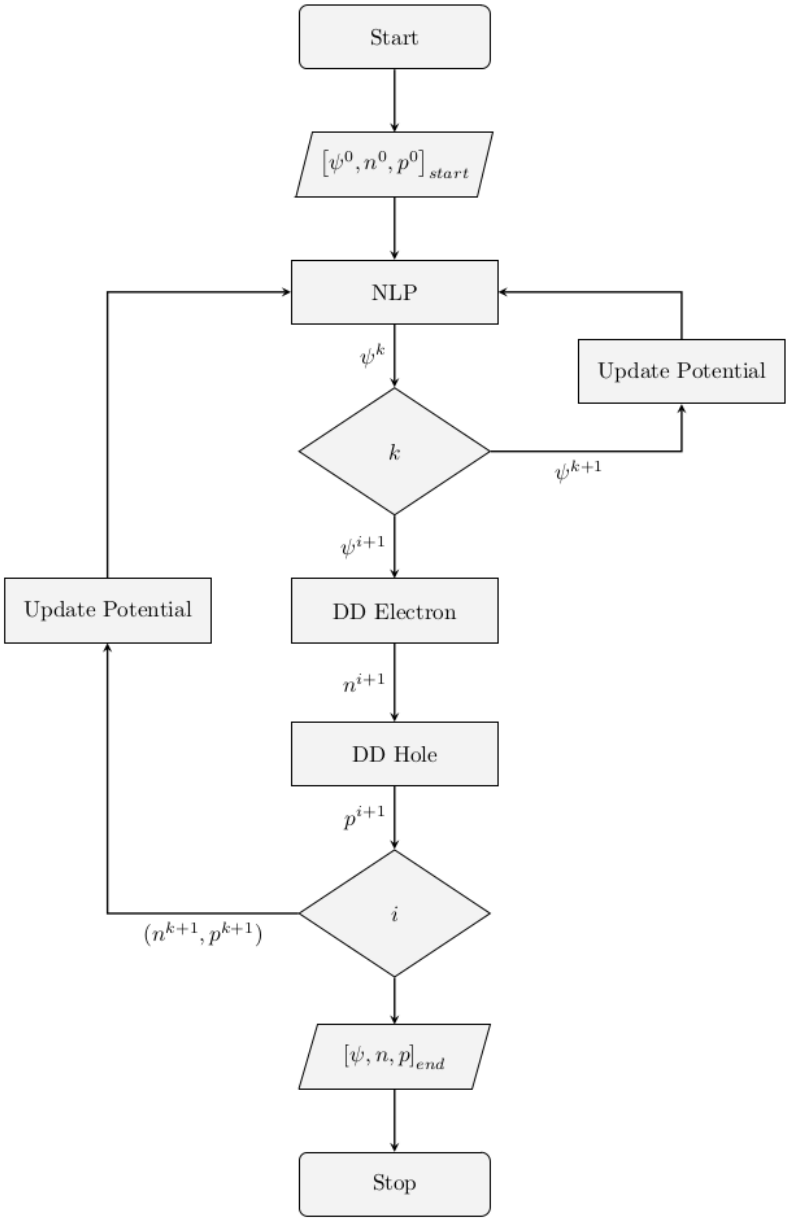

Fig. 2.2.2: Flowchart for the Gummel algorithm, where NLP and DD denote nonlinear Poisson's equation and drift-diffusion, respectively. The dependent variables ψ, n, and p denote the electric potential, the electron density, and the hole density.

Gummel's Method

H. K. Gummel devised an iterative method at the continuous level, which for Boltzmann statistics and drift-diffusion form, leads to alternating between solving linear differential equations for the electric potential and the charge carrier densities [Gummel]. The main idea is to move the nonlinearity to the Poisson equation. Therefore, given an suitable initial guess for the dependent variables $(\psi^{k=0}, n^{k=0}, p^{k=0})$, the electric potential at iteration $k+1$ can be computed from the Poisson equation. Given the the electric potential at iteration $k+1$, the charge carrier densities at iteration $k+1$ are obtained by successively solving the carrier continuity equations until the convergence tolerance in satisfied. The flowchart describing Gummel's algorithm is shown in Fig. 2.2.2. Gummel's method is stable an efficient for problems where the currents are small and the variations in the charge carrier densities are not extreme, i.e., the Van Roosbroeck equations are weakly coupled. Furthermore, the method is known to have a larger convergence region and a slower asymptotic convergence rate than Newtons's method.

Electro-thermomechanics

The following solution strategy is used to solve for the electric potential, carrier densities, temperature, and mechanical displacements of a semiconductor device:

1. Apply one of the solution methods in section *Solution Method* to solve for the carrier densities, electric potential, and temperature distributions in a semiconductor device.
2. Given a temperature distribution, solve for the displacement distribution in a semiconductor device. Recall that the governing equations describing the behavior of a thermo-mechanical system are coupled through the expressions describing the kinematics of the system, e.g., *the strain tensor*.

In the case of *linear elastic problems*, the displacements are computed by solving Eq.2.3.9. However, if large deformations and rotations are considered in the analysis of the electro-thermomechanical system, Eq.2.4.15 must be solved using a *multiplicative decomposition* for the deformation gradient.

Optimization

For steady state problems, the gradient of a nonlinear design criterion $f(\mathbf{u}, \mathbf{z})$ with respect to the vector design variables is computed using the solution method presented in the *Optimization* chapter, subsection *Elliptic*, where $\mathbf{u}$ and $\mathbf{z}$ are the vectors of state and design variables. The adjoint method for elliptic partial differential equations is applied to compute the vector of adjoint variables, i.e., Lagrange multipliers:

$$\begin{aligned} \boldsymbol{\lambda} &:= [\boldsymbol{\lambda}_\psi, \boldsymbol{\lambda}_n, \boldsymbol{\lambda}_p]^T \quad \text{(Isothermal Process)} \\ \boldsymbol{\lambda} &:= [\boldsymbol{\lambda}_\psi, \boldsymbol{\lambda}_n, \boldsymbol{\lambda}_p, \boldsymbol{\lambda}_\theta]^T \quad \text{(Non-isothermal Process).} \end{aligned} \tag{2.2.185}$$

The adjoint vector $\boldsymbol{\lambda}$ is needed to compute $df/d\mathbf{z}$ through Eq.3.2.6, where $df/d\mathbf{z}$ is the gradient of $f(\mathbf{u}, \mathbf{z})$ with respect to the vector of design variables $\mathbf{z}$. The solution method for elliptic partial differential equations is valid for both the isothermal and non-isothermal forms of the steady state drift-diffusion model.

For unsteady problems, $df/d\mathbf{z}$ is computed using the solution method presented in the *Optimization* chapter, subsection *Parabolic*. The adjoint method for parabolic partial differential equations is applied to compute the adjoint vector at every time step $\mathrm{n} > 0$:

$$\begin{aligned} \boldsymbol{\lambda}^{\mathrm{n}} &:= \left[\boldsymbol{\lambda}_\psi^{\mathrm{n}}, \boldsymbol{\lambda}_n^{\mathrm{n}}, \boldsymbol{\lambda}_p^{\mathrm{n}}\right]^T \quad \text{(Isothermal Process)} \\ \boldsymbol{\lambda}^{\mathrm{n}} &:= \left[\boldsymbol{\lambda}_\psi^{\mathrm{n}}, \boldsymbol{\lambda}_n^{\mathrm{n}}, \boldsymbol{\lambda}_p^{\mathrm{n}}, \boldsymbol{\lambda}_\theta^{\mathrm{n}}\right]^T \quad \text{(Non-isothermal Process).} \end{aligned} \tag{2.2.186}$$

The vector of adjoint variables $\boldsymbol{\lambda}^{\mathrm{n}}$ is computed at each time step to evaluate the contribution of n-th time step, i.e., t^{n}, to the calculation of $df/d\mathbf{z}$ through Eq.3.2.14. The solution method for parabolic partial differential equations is valid for both the isothermal and non-isothermal forms of the steady state drift-diffusion model.

In the case of *electro-thermo-elastostatics* physics, only steady state conditions are considered for the derivations. Thus, $df/d\mathbf{z}$ is computed using the solution method presented in the *Optimization* chapter, subsection *Elliptic*. The adjoint

method for elliptic partial differential equations is used to compute the vector of adjoint variables:

$$\boldsymbol{\lambda} := [\boldsymbol{\lambda}_\psi, \boldsymbol{\lambda}_n, \boldsymbol{\lambda}_p, \boldsymbol{\lambda}_\theta, \boldsymbol{\lambda}_d]^T. \tag{2.2.187}$$

A two-step solution strategy is employed to compute the vector of adjoint variables $\boldsymbol{\lambda}$. First, the adjoint system of equations for the mechanical physics is solved for $\boldsymbol{\lambda}_d$ as follows:

$$\boldsymbol{\lambda}_d = -\left(\frac{\partial \mathbf{R}_d(\mathbf{u}, \mathbf{z})}{\partial \mathbf{d}}\right)^{-T} \frac{\partial f(\mathbf{u}, \mathbf{z})}{\partial \mathbf{d}}, \quad \mathbf{x} \in \Lambda, \tag{2.2.188}$$

where $\mathbf{R}_d(\mathbf{u}, \mathbf{z})$ is the mechanical residual vector and $\mathbf{d}$ is the mechanical displacement vector. For *linear elasticity*, the mechanical residual is defined by Eq.2.3.9 and the kinematics are described by Eq.2.3.16. For *nonlinear elasticity*, the mechanical residual is defined by Eq.2.4.15 and the kinematics are described by Eq.2.4.26. The second step is to solve the adjoint system of equations for the non-isothermal form of the steady state drift-diffusion model for $\overline{\boldsymbol{\lambda}} = [\boldsymbol{\lambda}_\psi, \boldsymbol{\lambda}_n, \boldsymbol{\lambda}_p, \boldsymbol{\lambda}_\theta]^T$ as follows:

$$\overline{\boldsymbol{\lambda}} = (\mathbf{J}(\mathbf{u}, \mathbf{z}))^{-T} \mathbf{F}(\mathbf{u}, \mathbf{z}), \quad \mathbf{x} \in \Lambda. \tag{2.2.189}$$

The Jacobian $\mathbf{J}(\mathbf{u}, \mathbf{z})$ follows the form of Eq.2.2.183; however, it now depends on the vector of design variables $\mathbf{z}$. The vector $\mathbf{F}(\mathbf{u}, \mathbf{z})$ is defined as:

$$\mathbf{F}(\mathbf{u}, \mathbf{z}) := \begin{bmatrix} \partial f(\mathbf{u}, \mathbf{z})/\partial \psi \\ \partial f(\mathbf{u}, \mathbf{z})/\partial n \\ \partial f(\mathbf{u}, \mathbf{z})/\partial p \\ \partial f(\mathbf{u}, \mathbf{z})/\partial \theta + \boldsymbol{\lambda}_u^T (\partial \mathbf{R}_d(\mathbf{u}, \mathbf{z})/\partial \theta) \end{bmatrix}, \tag{2.2.190}$$

Once $\boldsymbol{\lambda}$ is computed by solving Eq.2.2.188 and Eq.2.2.189, the gradient of a design criterion with respect to the vector of design variables is computed as follows:

$$\frac{df(\mathbf{u}, \mathbf{z})}{d\mathbf{z}} = \frac{\partial f(\mathbf{u}, \mathbf{z})}{\partial \mathbf{z}} + \overline{\boldsymbol{\lambda}}^T \frac{\partial \mathbf{R}(\mathbf{u}, \mathbf{z})}{\partial \mathbf{z}} + \boldsymbol{\lambda}_u^T \frac{\partial \mathbf{R}_u(\mathbf{u}, \mathbf{z})}{\partial \mathbf{z}}. \tag{2.2.191}$$

The residual $\mathbf{R}(\mathbf{u}, \mathbf{z})$ follows the form of Eq.2.2.180; however, it depends on the vector of design variables $\mathbf{z}$.

2.3 Linear Elasticity

Linear elasticity describes how a solid object deforms and becomes internally stressed due to external forces. The fundamental assumptions of linear elasticity are strains are small, stresses and strains are linearly related, and stresses are below the material yield point [Hughes].

2.3.1 Kinematics

The strain tensor for linear elasticity is defined as:

$$\epsilon_{ij} = \frac{1}{2}\left(\frac{\partial u_i}{\partial x_j} + \frac{\partial u_j}{\partial x_i}\right), \tag{2.3.1}$$

where $i, j = 1, \ldots, d$ and the dimension is defined as $d \in \{1, 2, 3\}$. The i-th displacement and coordinate are given by u_i and x_i, respectively.

2.3.2 Kinetics

The elastic energy potential; i.e., strain energy potential, for a linear elastic material is defined as:

$$W(u_i) = \frac{1}{2}\epsilon_{ij}\, C_{ijkl}\, \epsilon_{kl}, \tag{2.3.2}$$

where $k, l = 1, \ldots, d$, C_{ijkl} is the fourth-order elasticity tensor; i.e., stiffness tensor. The infinitesimal strain tensor, ϵ_{kl}, is given by Eq.2.3.1.

In linear elasticity, it is safe to assume that the stress tensor derives from Eq.2.3.2 as follows:

$$\sigma_{ij} = \frac{\partial W}{\partial \epsilon_{ij}} = C_{ijkl}\epsilon_{kl}, \tag{2.3.3}$$

where σ_{ij} is the Cauchy stress tensor. The stress tensor in linear elasticity is a generalization of Hooke's law to three-dimensional continuum. Eq.2.3.3 implies

$$C_{ijkl} = \frac{\partial W}{\partial \epsilon_{ij} \partial \epsilon_{kl}}. \tag{2.3.4}$$

Therefore, the elasticity tensor must be symmetric under interchange of the first and second pairs of indices:

$$C_{ijkl} = C_{klij}. \tag{2.3.5}$$

The elasticity tensor has additional symmetry properties that follow from the constitutive equation, Eq.2.3.3. The symmetry of the stress and strain tensors implies:

$$C_{ijkl} = C_{jikl} \quad \text{and} \quad C_{ijkl} = C_{jilk}. \tag{2.3.6}$$

The symmetry properties listed in Eq.2.3.5 and Eq.2.3.6 reduce the number of independent components in the elasticity tensor from 81 to 21. The number of independent components can be further reduced based on additional symmetry properties of a material.

2.3.3 Equilibrium of Stresses

The stress components in any continuum are constrained by the requirement that all parts of the body obey Newton's law of motion. Applying this condition to an infinitesimally small rectangular element of material, the following

$$\frac{\partial \sigma_{ij}}{\partial x_j} + b_i = \rho \frac{\partial^2 u_i}{\partial t^2} \tag{2.3.7}$$

where b_i represents the components of a body force vector $\mathbf{b}$ per unit volume, ρ is the material density, and t is time. The basic postulate of elastostatics is that the loading rate is sufficiently small for the acceleration term $\partial^2 u_i / \partial t^2$ to be neglected, leading to the equilibrium equation:

$$\frac{\partial \sigma_{ij}}{\partial x_j} + b_i = 0. \tag{2.3.8}$$

2.3.4 Weak Formulation

Static equilibrium is achieved when the net force acting on a body is zero. The net force is defined as the sum of all the forces, internal and external, acting on a body Ω with boundary Γ. Let $H^1(\Omega)$ be the Sobolev space of weakly differentiable functions and $H^1_D(\Omega) = \{w_i \in H^1(\Omega) \mid w_i = 0 \text{ on } \Gamma_D\}$, with Γ_D defined as the Dirichlet boundary. This statement can be mathematically expressed using the principle of virtual work, introducing an arbitrary, variational displacement field w_i and integrating over the volume:

$$R^u_i(u_i) = \int_\Omega \sigma_{ij} w_{ij} \, d\Omega - \int_{\Gamma_\tau} \bar{\tau}_i w_i \, d\Gamma - \int_{\Gamma_p} \bar{p} w_i \, d\Gamma - \int_\Omega b_i w_i \, d\Omega = 0, \quad w_i \in H^1(\Omega), \tag{2.3.9}$$

where w_{ij} is an arbitrary variational strain tensor, $\bar{\tau}_i$ is a prescribed traction force acting on surface Γ_τ, $\bar{p}$ is a prescribed force per unit area (e.g., pressure) on boundary $\Gamma_p = \Gamma \setminus \Gamma_\tau$, and b_i is a body force, i.e., gravity force. The product rule was used in the derivation of Eq.2.3.9 to reduce the derivative order on an expression in conjunction with the divergence theorem.

2.3.5 Constitutive Relations

Isotropic Materials

Isotropic materials deformed equally in all directions regardless of the direction in which the force(s) is applied. The Cauchy stress tensor may be computed using the following fourth-order elasticity tensor:

$$C_{ijkl} = K\delta_{ij}\delta_{kl} + \mu\left(\delta_{ik}\delta_{jl} + \delta_{il}\delta_{jk} - \frac{2}{3}\delta_{ij}\delta_{kl}\right), \tag{2.3.10}$$

where δ_{ij} is the Kronecker delta, K is the bulk modulus, and μ is the shear modulus. The material constitutive relation may now be written as:

$$\sigma_{ij} = \lambda\delta_{ij}\epsilon_{kk} + 2\mu\epsilon_{ij}, \tag{2.3.11}$$

The material constant λ can be computed from the following relationship:

$$\lambda = K - \frac{2}{3}\mu. \tag{2.3.12}$$

Table 2.3.1: Voigt index mapping employed in two-dimensional problems

Format	C1	C2	C3
ij	11	22	12,21
α	1	2	3

Table 2.3.2: Voigt index mapping employed in three-dimensional problems

Format	C1	C2	C3	C4	C5	C6
ij	11	22	33	23,32	13,31	12,21
α	1	2	3	4	5	6

Anisotropic Materials

In three-dimensional problems, Voig notation permits recasting the fourth-order elasticity tensor as a second-order tensor of the form:

$$C_{ijkl} \Rightarrow C_{\alpha\beta} = \begin{bmatrix} C_{11} & C_{12} & C_{13} & C_{14} & C_{15} & C_{16} \\ C_{21} & C_{22} & C_{23} & C_{24} & C_{25} & C_{26} \\ C_{31} & C_{32} & C_{33} & C_{34} & C_{35} & C_{36} \\ C_{41} & C_{42} & C_{43} & C_{44} & C_{45} & C_{46} \\ C_{51} & C_{52} & C_{53} & C_{54} & C_{55} & C_{56} \\ C_{61} & C_{62} & C_{63} & C_{64} & C_{65} & C_{66} \end{bmatrix} \tag{2.3.13}$$

The second order tensor presented in Eq.2.3.13 is symmetric; therefore, there are at most 21 independent elements of $C_{\alpha\beta}$.

The simplest anisotropic case is the cubic symmetric case, which has three independent elements. The seond-order elasticity tensor for materials exhibiting cubic symmetry is defined as:

$$C_{ijkl} \Rightarrow C_{\alpha\beta} = \begin{bmatrix} C_{11} & C_{12} & C_{12} & 0 & 0 & 0 \\ C_{12} & C_{11} & C_{12} & 0 & 0 & 0 \\ C_{12} & C_{12} & C_{11} & 0 & 0 & 0 \\ 0 & 0 & 0 & C_{44} & 0 & 0 \\ 0 & 0 & 0 & 0 & C_{44} & 0 \\ 0 & 0 & 0 & 0 & 0 & C_{44} \end{bmatrix} \tag{2.3.14}$$

The orthotropic case has nine independent elements. The seond-order elasticity tensor for orthotropic materials is defiend as:

$$C_{ijkl} \Rightarrow C_{\alpha\beta} = \begin{bmatrix} C_{11} & C_{12} & C_{13} & 0 & 0 & 0 \\ C_{12} & C_{22} & C_{23} & 0 & 0 & 0 \\ C_{13} & C_{23} & C_{33} & 0 & 0 & 0 \\ 0 & 0 & 0 & C_{44} & 0 & 0 \\ 0 & 0 & 0 & 0 & C_{55} & 0 \\ 0 & 0 & 0 & 0 & 0 & C_{66} \end{bmatrix} \tag{2.3.15}$$

There are other anisotropic cases in the literature, but they are not presented in this manual. The user is encourage to consult the vast literature in anisotropic materials if interested.

2.3.6 Thermo-elastostatics

The kinematics for thermo-elastic systems is described by the following relationship:

$$\epsilon_{ij} = \epsilon^u_{ij} + \epsilon^\theta_{ij}, \tag{2.3.16}$$

where the total strain tensor is the sum the elastic strain ϵ^u_{ij} and the thermal strain ϵ^θ_{ij}. The elastic strain is computed from Eq.2.3.1 while the thermal strain is computed from:

$$\epsilon^\theta_{ij} = \alpha_{ij}\delta_{ij}\left(\theta - \theta_0\right), \tag{2.3.17}$$

where α_{ij} is the coefficient of thermal expansion θ is the temperature at the evaluation point, and θ_0 is the reference temperature. The unit of measurement for the coefficient of thermal expansion is the inverse of temperature, e.g, K^{-1}. The coefficient of thermal expansion measures the rate at which a material deforms with temperature. The reference temperature θ_0 is the temperature at which the thermal strains are zero, i.e., $\epsilon^\theta_{ij} = 0$. Finally, the Cauchy stress tensor σ_{ij} is computed from Eq.2.3.3, where the strain tensor is computed from Eq.2.3.16.

The following solution strategy is employed to solve for the temperature and displacement fields of thermo-elastic structures:

1. Solve the *thermostatics equation*:

   $\mathbf{R}^\theta = \int_\Omega \mathbf{q}\cdot\nabla w \, d\Omega - \int_\Omega Hw \, d\Omega - \int_\Gamma q^0 w \, d\Gamma = 0, \quad \in w \in H^1(\Omega),$

   for the temperature $\theta \in H^1(\Omega)$, and

2. Solve the *elastostatics equation*:

   $R^u_i = \int_\Omega \sigma_{ij} w_{ij} \, d\Omega - \int_{\Gamma_\tau} \bar{\tau}_i w_i \, d\Gamma - \int_{\Gamma_p} \bar{p} w_i \, d\Gamma - \int_\Omega b_i w_i \, d\Omega = 0, \quad w_i \in H^1(\Omega),$

   for the displacements $u_i \in H^1(\Omega)$‘. Recall that the Cauchy stress tensor σ_{ij} is computed using Eq.2.3.3 and the total strain tensor ϵ_{ij} is computed using Eq.2.3.16.

2.3.7 Boundary Conditions

Boundary conditions for mechanical physics can be specified as:

- a prescribed displacement vector $\mathbf{u} = \mathbf{u}(\mathbf{x}, t)$ on boundary Γ_u,
- a prescribed traction force vector $\bar{\boldsymbol{\tau}}(\mathbf{x}, t)$ on boundary Γ_τ,
- a prescribed body force vector $\mathbf{b}(\mathbf{x}, t)$,
- a prescribed pressure force $\bar{p}(\mathbf{x}, t)$ on boundary Γ_p.

In addition to the boundary conditions listed above for mechanical physics, the following boundary conditions can be specified for thermo-mechanical physics:

- a prescribed temperature $\theta = \theta(\mathbf{x}, t)$

- a prescribed surface heat flux $q_0 = q_0(\mathbf{x}, t)$
- convective heat transfer on surface Γ_c, which is defined as:

  $q_c = q_c(\mathbf{x}, t) = h(\theta - \theta_0)$,

  where $h = h(\mathbf{x}, t)$ is the heat transfer coefficient and $\theta_0 = \theta_0(\mathbf{x}, t)$ is the sink temperature.

If the problem does not depend on time, which is the case for elastostatics thermo-elastistatics problems, time is set to zero; i.e. $t = 0$.

2.3.8 Optimization

The gradient of a nonlinear design criterion with respect to the vector design variables $\mathbf{z}$ is computed using the solution method for elliptic partial differential equations presented in the *Optimization* chapter, subsection *Elliptic*. The solution method applies to both elastostatics and thermo-elastostatics physics.

2.4 Nonlinear Elasticity

The sources of nonlinearities in a mechanical analysis can be due to material and or geometric nonlinearities. This chapter introduces the governing equations describing the behavior of mechanical systems experiencing large deformations and rotations. This physical phenomenon requires modeling of the second-order terms in the strain calculations. This source of nonlinearities in the system is known as geometric nonlinearity.

2.4.1 Kinematics

The motion of a body is defined as

$$x_i = \phi_i(X_j, t), \tag{2.4.1}$$

where the coordinates x_i give the spatial position of the material coordinates X_i at time t. The function $\phi_i(X_j, t)$ maps the reference (undeformed) configuration into the current (deformed) configuration at time t. This function is often call the mapping from the reference configuration to the current configuration.

The displacement of a material point is given by the difference between the current position and the original position:

$$u_i = \phi_i(X_j, t) - X_i = x_i - X_i, \tag{2.4.2}$$

where the mapping function definition, Eq.2.4.1, has been used in Eq.2.4.2.

A relevant quantity for the characterization of mechanical deformation is the deformation gradient. The deformation gradient is defined as:

$$F_{ij} = \frac{\partial x_i}{\partial X_j}, \tag{2.4.3}$$

where $i, j = 1, \ldots, d$, and the dimension $d \in \{1, 2, 3\}$. The deformation gradient is the Jacobian matrix of the motion $\phi_i(X_j, t)$. The determinant of Eq.2.4.3 is defined as:

$$J = \det(\mathbf{F}) \tag{2.4.4}$$

The determinant of the deformation gradient J is used to relate integrals in the deformed and undeformed configurations.

The strain measure is defined by the Green strain tensor:

$$E_{ij} = \frac{1}{2}\left(\frac{\partial u_i}{\partial X_j} + \frac{\partial u_j}{\partial X_i} + \frac{\partial u_k}{\partial X_i}\frac{\partial u_k}{\partial X_j}\right), \tag{2.4.5}$$

where $i, j, k = 1, \ldots, d$. There are many strain measures defined in the literature for nonlinear continuum mechanics. In some applications, a strain measure different to Eq.2.4.5 may be used. However, it must vanish for any rigid body motion, and in particular for rigid body rotation.

2.4.2 Kinetics

Various stress measures can be defined in nonlinear mechanical problems: Cauchy stress, σ_{ij}, Nominal stress, P_{ij}, and second Piola-Kirchhoff stress, S_{ij}. The stresses are defined by the Cauchy law as follows:

$$n_j \sigma_{ij} \, d\Gamma = \tau_i \, d\Gamma, \tag{2.4.6}$$

where τ_i is the traction on the deformed configuration boundary $d\Gamma$ and n_j is the $j-th$ component of the normal vector acting on $d\Gamma$. The counterpart stress measure for the Cauchy stress in the undeformed (reference) configuration is the first Piola-Kirchhoff P_{ij}, which is defined as:

$$n_j^0 P_{ij} \, d\Gamma^0 = \tau_i^0 \, d\Gamma^0, \tag{2.4.7}$$

where τ_i^0 is the traction on the reference configuration boundary $d\Gamma^0$ and n_j^0 is the $j-th$ component of the normal vector acting on $d\Gamma^0$. The second Piola-Kirchhoff (2PK) stress is defined as:

$$n_j^0 S_{ij} \, d\Gamma^0 = F_{ik}^{-1} t_k^0 \, d\Gamma^0. \tag{2.4.8}$$

The second Piola-Kirchhoff stress, Eq.2.4.8, differs from the nominal stress, Eq.2.4.7, in that it is transformed by F_{ik}^{-1}. In contrast to the nominal stress, the second Piola-Kirchhoff stress is made symmetric by the transformation.

The different stress measures are interrelated by functions of the deformation. Table 2.4.1 shows the transformations between the different stress measures.

Table 2.4.1: Stress Transformations

	Cauchy stress	Nominal stress	2PK stress
σ_{ij}		$J^{-1} F_{ik} S_{kj}$	$J^{-1} F_{ik} S_{kl} F_{lj}^T$
P_{ij}	$J F_{ik}^{-1} \sigma_{kj}$		$S_{ik} F_{kj}^T$
S_{ij}	$J F_{ik}^{-1} \sigma_{kl} F_{lj}^{-T}$	$P_{ik} F_{kj}^{-T}$	

The relationships introduced in Table 2.4.1 can be derived by using Eq.2.4.6-Eq.2.4.8 and Nanson's relation. The Nanson relation relates the current normal to the reference normal by:

$$n_i \, d\Gamma = J n_j^0 F_{ji}^{-1} \, d\Gamma^0 \tag{2.4.9}$$

2.4.3 Equilibrium of Stresses

The stress components in any continuum are constrained by the requirement that all parts of the body obey Newton's law of motion. Applying this condition to an infinitesimally small rectangular element of material, the following

$$\frac{\partial P_{ji}}{\partial X_j} + \rho_0 B_i = \rho_0 \frac{\partial^2 u_i}{\partial t^2}, \tag{2.4.10}$$

where t denotes time and B_i is the $i-th$ component of the body force vector per unit mass. The $i-th$ component of the body force vector per unit volume is defined as:

$$b_i = \rho_0 B_i. \tag{2.4.11}$$

The material density in the undeformed configuration is defined as:

$$\rho_0 = \rho J, \tag{2.4.12}$$

where ρ is the material density in the deformed configuration and $J = \det(\mathbf{F})$. The Lagrangian description of the mass conservation equation, which is defined as:

$$\int_{\Omega^0} (\rho J - \rho_0) \, d\Omega^0, \tag{2.4.13}$$

was used to derive Eq.2.4.12. The basic postulate of elastostatics is that the loading rate is sufficiently small for the acceleration term $\partial^2 u_i/\partial t^2$ to be neglected, leading to the following equilibrium equation:

$$\frac{\partial P_{ji}}{\partial X_j} + b_i = 0. \tag{2.4.14}$$

2.4.4 Weak Formulation

The balance of linear momentum within the undeformed domain Ω^0 with boundary Γ^0 is described by the *static equilibrium of the internal and external forces*. Let $H^1(\Omega^0)$ be the Sobolev space of weakly differentiable functions and $H^1_D(\Omega^0) = \{w_i \in H^1(\Omega^0) \mid w_i = 0 \text{ on } \Gamma^0_D\}$, with Γ^0_D defined as the Dirichlet boundary. A total Lagrangian finite element formulation is applied to derive the kinematically admissible displacements. The variational form of governing equation using a total Lagrangian formulation is given by:

$$R^u_i = \int_{\Omega^0} \left(\delta F_{ij} P_{ji} - w_i b_i\right)\, d\Omega^0 - \int_{\Gamma^0_\tau} w_i \bar{\tau}_i \, d\Gamma^0 - \int_{\Gamma^0_p} w_i \bar{p} \, d\Gamma^0 = 0, \quad w_i \in H^1(\Omega^0) \tag{2.4.15}$$

where δF_{ij} is an arbitratry variational deformation gradient. $F_{ij} = \partial x_i/\partial X_j$ is the total deformation gradient tensor with $x_i = u_i + X_i$ defining the relationship between the spatial coordinates x_i and X_j in the deformed and undeformed configurations, respectively. The kinematically admissible displacements and test functions are respectively denoted by u_i and w_i. The first Piola-Kirchhoff stress tensor in the undeformed configuration is represented by P_{ji}. $\bar{u}_i$ is the prescribed displacement field on the undeformed boundary Γ^0_u while the traction force $\bar{\tau}_i$ is prescribed on the undeformed boundary Γ^0_τ. The pressure force $\bar{p}$ is prescribed on undeformed boundary $\Gamma^0_p = \Gamma^0 \setminus \Gamma^0_\tau$.

2.4.5 Constitutive Relations

The material response of a body is characterized by a constitutive relation that gives the stress as a function of the deformation experienced by the body. In a displacement based finite element formulation, the constitutive relation is used to represent stress, increments, or strain increments, in terms of displacement increments.

Hyperelastic Materials

Hyperelastic materials are elastic materials where the work done in the material is independent of the load path. Hyperleastic materials are characterized by the exsitance of a strain energy function denoting an energy potential for stress. Hyperelastic materials can undergo large deformations while remaining elastic. Thus, a hyperelastic material can return to its original shape when the load is removed.

Saint Venant - Kirchhoff

The simplest hyperelastic material model is the Saint Venant - Kirchhoff model. The Saint Venant - Kirchhoff material model can be used in problems were the effects of large deformations are primarily due to rotations. The Saint Venant - Kirchhoff material model is a generalization of Hooke's law for linear elasticity. The Saint Venant - Kirchhoff model accomplishes this through the use of the second-order Green strain tensor:

$$E_{ij} = \frac{1}{2}\left(C_{ij} - \delta_{ij}\right), \tag{2.4.16}$$

where C_{ij} is the right Cauchy-Green tensor. The strain energy function for a Saint Venant - Kirchhoff material model is defined as:

$$W(E) = \frac{1}{2} E_{ij} C_{ijkl} E_{kl}, \tag{2.4.17}$$

where the fourth-order elasticity tensor C_{ijkl} is defined as:

$$C_{ijkl} = \lambda_0 \delta_{ij}\delta_{kl} + \mu_0 \left(\delta_{ik}\delta_{jl} + \delta_{il}\delta_{kj}\right). \tag{2.4.18}$$

The constants λ_0 and μ_0 are the Lame constants. Recall that $K - \frac{2}{3}\mu_0$, where K is the bulk modulus and μ_0 is the chear modulus. The second Piola-Kirchhoff stress for a Saint Venant - Kirchhoff material is defined as:

$$S_{ij} = C_{ijkl} E_{kl}, \tag{2.4.19}$$

where second-order Green strain tensor E_{kl} and the fourth-order elasticity tensor are defined by Eq.2.4.16 and Eq.2.4.18, respectively.

Neo-Hookean

A neo-Hookean material is a hyperelastic material model that can be used for predicting the nonlinear stress - strain behavior of elastic materials undergoing large deformations. In contrast to linear elastic materials, the stress - strain curve of a neo-Hookean material is nonlinear. The stress - strain is initially linear, but at a certain point the stress - strain curve plateaus. The strain energy function for a compressible neo-Hookean material that is isotropic with respect to the reference configuration is defined as:

$$W(\mathbf{C}) = \frac{1}{2}\lambda_0 \left(\log(J)\right)^2 - \mu_0 \log(J) + \frac{1}{2}\mu_0 \left(C_{ii} - 3\right), \tag{2.4.20}$$

where $\mathbf{C}$ is the right Cauchy-Green tensor, which is defined as:

$$C_{ij} = F_{ki} F_{kj}. \tag{2.4.21}$$

The parameters λ_0 and μ_0 are the Lame constants and C_{ii} is the trace of the right Cauchy-Green tensor.

The second Piola-Kirchhoff stress for a neo-Hookean material is given by:

$$S_{ij} = \lambda_0 [\log(J) C^{-1}_{ij} + \mu_0 \left(\delta_{ij} - C^{-1}_{ij}\right). \tag{2.4.22}$$

where $J = \det(\mathbf{F})$. The fourth-order material elasticity tensor for a neo-Hookean material is defined as:

$$C_{ijkl} = \lambda C^{-1}_{ij} C^{-1}_{kl} + \mu \left(C^{-1}_{ik} C^{-1}_{jl} + C^{-1}_{il} C^{-1}_{kj} \right), \tag{2.4.23}$$

where $\lambda = \lambda_0$ and $\mu = \mu_0 - \lambda \log(J)$.

2.4.6 Thermo-elastostatics

The kinematics of thermo-mechanical structures is described by a multiplicative decomposition of the total deformation gradient. The multiplicative decomposition separates the total deformation into a purely mechanical contribution F^u_{ij} and a purely thermal contribution F^θ_{ij}. An intermediate material configuration $\tilde{\Omega}$ is introduced between the current configuration Ω and the reference configuration Ω^0 to characterize the kinematics of thermo-mechanical structures. The intermediate material configuration is a virtual state conceptually introduced by isothermal elastic distressing of the current configuration to a stress-free material state. Mathematically, the multiplicative decomposition of the deformation gradient is defined as:

$$F_{ij} = F^u_{ik} F^\theta_{kj}. \tag{2.4.24}$$

The thermo-mechanical deformation gradient Eq.2.4.24 linearly maps a coordinate X_i on the reference configuration to a coordinate x_i on the deformed configuration. The thermal deformation gradient in Eq.2.4.24 is defined by:

$$F^\theta_{ij} = \left[1 + \alpha \left(\theta - \theta_0\right)\right] \delta_{ij}, \tag{2.4.25}$$

The thermal deformation gradient maps a coordinate X_i on the reference configuration to a coordinate $\tilde{x}_i \in \tilde{\Omega}$ on the intermediate configuration. The mechanical deformation gradient:

$$F^u_{ij} = F_{ik} \left(F^\theta_{kj}\right)^{-1}, \tag{2.4.26}$$

maps a coordinate $\tilde{x}_i$ on the intermediate configuration to a coordinate x_i on the thermo-elastic deformed configuration. The temperature θ is computed by solving the thermostatics equations introduced in Eq.2.1.12. Once the temperature distribution in a body is determined, Eq.2.4.15 is solved to compute the displacements.

The following solution strategy is implemented to solve for the temperature and displacement fields of structures subjected to thermal and mechanical forces:

1. Solve the *thermostatics equation*:

   $\mathbf{R}^{\theta} = \int_{\Omega} \nabla w \cdot \mathbf{q} \, d\Omega - \int_{\Omega} wH \, d\Omega - \int_{\Gamma} wq_0 \, d\Gamma = 0, \quad w \in H^1(\Omega),$

   for the temperatures $\theta \in H^1(\Omega)$, and

2. Solve the *nonlinear mechanical equation*:

   $R_i^u = \int_{\Omega^0} \left(\delta F_{ij} P_{ji} - w_i b_i\right) \, d\Omega^0 - \int_{\Gamma_\tau^0} w_i \bar{\tau}_i \, d\Gamma^0 - \int_{\Gamma_p^0} w_i \bar{p} \, d\Gamma^0 = 0, \quad w \in H^1(\Omega^0),$

   for the displacement $u_i \in H^1(\Omega^0)$.

2.4.7 Boundary Conditions

Boundary conditions for Eq.2.4.15 can be specified as:

- a prescribed displacement $\bar{u}_i = \bar{u}_i(\mathbf{x}, t)$ on boundary Γ_0
- a prescribed surface traction per unit area $\bar{\tau}_i = \bar{\tau}_i(\mathbf{x}, t)$ on boundary Γ_τ^0
- a body force per unit mass $B_i = B_i(\mathbf{x}, t)$
- a prescribed pressure on $\bar{p}(\mathbf{x}, t)$ on boundary Γ_p^0
- a prescribed follower pressure $\bar{p} = \bar{p}(\mathbf{x}, t)$ on Γ_p^0, which is defined as:

$$R_i^p = \int_{\Gamma_p^0} w_i J F_{ji}^{-1} \left(n_j^0 \bar{p}\right) \, d\Gamma^0, \tag{2.4.27}$$

Eq.2.4.9 was used in Eq.2.4.27 to transform the normal vector on the undeformed configuration to the deformed configuration. In addition to the boundary conditions listed above for nonlinear mechanical physics, the following boundary conditions can be specified for nonlinear thermo-mechanical physics:

- a prescribed temperature $\theta = \theta(\mathbf{x}, t)$
- a prescribed surface heat flux $q_0 = q_0(\mathbf{x}, t)$
- a prescribed surface convection, which is defined as:

  $q_c = q_c(\mathbf{x}, t) = h(\theta - \theta_0),$

  where $h = h(\mathbf{x}, t)$ is the heat transfer coefficient and $\theta_0 = \theta_0(\mathbf{x}, t)$ is the sink temperature.

If the problem does not depend on time, which is the case for nonlinear elastostatics and thermo-elastistatics problems, time is set to zero; i.e. $t = 0$.

2.4.8 Optimization

The gradient of a nonlinear design criterion with respect to the vector design variables $\mathbf{z}$ is computed using the solution method for elliptic partial differential equations presented in the *Optimization* chapter, subsection *Elliptic*. The solution method applies to both elastostatics and thermo-elastostatics physics.

CHAPTER

THREE

OPTIMIZATION

The *Optimization* chapter describes the foundational optimizaton concepts used to derive the simulation-driven design formulations. In addition, the *Optimization* chapter presents the mathematical expressions for the design criteria implemented in the Morphorm software.

3.1 Introduction

A general optimization framework is implemented in the Morphorm software to solve simulation-based design optimization problems constrained by Partial Differential Equation (PDE) and other linear and nonlinear constraints. Automatic differentiation methods are used to compute the Jacobian matrices and partial derivatives with respect to the physical responses and design parameters. The subsequent sections introduce the general framework, design criteria, and methods used for simulation-based design.

3.2 Foundations

3.2.1 Adjoint Method

The theoretical foundations for the adjoint method are introduced in this section for gradeint-based optimization problems constrained by *elliptic* or *parabolic* partial differential equations (PDE).

Elliptic

Consider the following PDE-constrained optimization problem:

$$\min_{\mathbf{z}\in\mathbb{R}^{N_z}} \quad f(\mathbf{u},\mathbf{z}) \quad s.t. \quad \mathbf{R}(\mathbf{u},\mathbf{z})=0, \quad \underline{z}_i \le z_i \le \bar{z}_i \quad i=1,\ldots,N_z, \tag{3.2.1}$$

where the vector $\mathbf{z}$ contains the N_z design variables. The parameters $\underline{z}_i$ and $\bar{z}_i$ imposed lower and upper bounds on the i-th design variable z_i, respectively. The vector $\mathbf{u} \in \mathbb{R}^{N_u}$ solves the partial differential equation (PDE) describing the physical system given a fixed environment, material definition, and configuration. The vector $\mathbf{u}$ implicitly depends on $\mathbf{z}$. The objective function $f\left(\mathbf{u},\mathbf{z}\right)$ and residual vector $\mathbf{R}(\mathbf{u},\mathbf{z})$ complete the optimization formulation. Although the PDE-constrained optimization formulation in Eq.3.2.1 does not include inequality constraints, the Morphorm optimization framework supports enforcement of linear and nonlinear inequality constraints in an optimization problem.

The method of Lagrange multipliers, i.e., adjoint method, is applied to find a local minimum of Eq.3.2.1. The method of Lagrange multipliers states that there exists a vector of Lagrange multipliers λ_0 such that $(\mathbf{u}_0,\mathbf{z}_0,\lambda_0)$ is the stationary point of the Lagrangian:

$$\mathcal{L}\left(\mathbf{u},\mathbf{z};\lambda\right) = f\left(\mathbf{u},\mathbf{z}\right) + \lambda^T \mathbf{R}\left(\mathbf{u},\mathbf{z}\right), \tag{3.2.2}$$

where the stationary point of Eq.3.2.2 is defined as:

$$\frac{\partial f}{\partial \mathbf{z}} + \lambda^T \frac{\partial \mathbf{R}}{\partial \mathbf{z}} + \left(\frac{\partial f}{\partial \mathbf{u}} + \lambda^T \frac{\partial \mathbf{R}}{\partial \mathbf{u}}\right)\frac{\partial \mathbf{u}}{\partial \mathbf{z}} = 0, \tag{3.2.3}$$

where the dependencies on the state, $\mathbf{u}$, and the control, $\mathbf{z}$, vectors have been dropped from Eq.3.2.3 for convenience. Eq.3.2.3 is satisfied if the following condition is met:

$$\frac{\partial f\left(\mathbf{u},\mathbf{z}\right)}{\partial \mathbf{u}}+\lambda^{T}\frac{\mathbf{R}\left(\mathbf{u},\mathbf{z}\right)}{\partial \mathbf{u}}=0. \tag{3.2.4}$$

The Lagrange multipliers satisfying the stationary condition, Eq.3.2.3, are the solution to Eq.3.2.4, which yields:

$$\begin{aligned}\frac{\partial f\left(\mathbf{u},\mathbf{z}\right)}{\partial \mathbf{u}}+\left(\frac{\mathbf{R}\left(\mathbf{u},\mathbf{z}\right)}{\partial \mathbf{u}}\right)^{T}\lambda =&0\\ \lambda =&-\left(\frac{\mathbf{R}\left(\mathbf{u},\mathbf{z}\right)}{\partial \mathbf{u}}\right)^{T}\frac{\partial f\left(\mathbf{u},\mathbf{z}\right)}{\partial \mathbf{u}}.\end{aligned} \tag{3.2.5}$$

Once Eq.3.2.5 is solved for λ, the gradient of the objective function is computed from:

$$\frac{df}{d\mathbf{z}}=\frac{\partial f\left(\mathbf{u},\mathbf{z}\right)}{\partial \mathbf{z}}+\lambda^{T}\frac{\mathbf{R}\left(\mathbf{u},\mathbf{z}\right)}{\partial \mathbf{z}}. \tag{3.2.6}$$

Similarly, the gradient of any nonlinear constraint function with respect to the design variables can be computed using the method of Lagrange multipliers.

Parabolic

Consider the following PDE-constrained optimization problem:

$$\begin{aligned}\min_{\mathbf{z}\in\mathbb{R}^{N_{\mathbf{z}}}}\quad & f(\mathbf{u}^{n},\mathbf{u}^{n-1},\mathbf{z})\\ s.t.\quad &\\ \mathbf{R}(\mathbf{u}^{n},\mathbf{u}^{n-1},\mathbf{z})&=0,\\ \underline{z}_{i}\leq z_{i}\leq \bar{z}_{i}\quad & i=1,\ldots,N_{\mathbf{z}},\end{aligned} \tag{3.2.7}$$

where the vector $\mathbf{z}$ contains the $N_{\mathbf{z}}$ design variables. The parameters $\underline{z}_i$ and $\bar{z}_i$ imposed lower and upper bounds on the i-th design variable z_i, respectively. The vectors of state variables $\mathbf{u}^n \in \mathbb{R}^{N_u}$ and $\mathbf{u}^{n-1} \in \mathbb{R}^{N_u}$ at time cycles n and $n-1$ solve the partial differential equation describing the physical system for a fixed environment, material definition, and configuration. The objective function $f\left(\mathbf{u}^n,\mathbf{u}^{n-1},\mathbf{z}\right)$ and residual vector $\mathbf{R}(\mathbf{u}^n,\mathbf{u}^{n-1},\mathbf{z})$ complete the optimization formulation. Although the optimization formulation in Eq.3.2.7 does not model inequality constraints, the Morphorm optimization framework supports enforcement of linear and nonlinear inequality constraints.

The method of Lagrange multipliers states that there exists a vector of Lagrange multipliers λ_0 such that $\left(\mathbf{u}_0^n,\mathbf{u}^{n-1},\mathbf{z}_0,\lambda_0\right)$ is the stationary point of the Lagrangian:

$$\mathcal{L}\left(\mathbf{u}^{n},\mathbf{u}^{n-1},\mathbf{z};\lambda\right)=f\left(\mathbf{u}^{n},\mathbf{u}^{n-1},\mathbf{z}\right)+\lambda^{T}\mathbf{R}\left(\mathbf{u}^{n},\mathbf{u}^{n-1},\mathbf{z}\right), \tag{3.2.8}$$

where the stationary point of Eq.3.2.8 is defined as:

$$\begin{aligned}&\frac{\partial\mathcal{L}\left(\mathbf{u}^{n},\mathbf{u}^{n-1},\mathbf{z};\lambda\right)}{\partial \mathbf{z}}=\\ &\frac{\partial f(\mathbf{u}^{n},\mathbf{u}^{n-1},\mathbf{z})}{\partial \mathbf{z}}+\sum_{n=1}^{N_t}\left(\frac{\partial f(\mathbf{u}^{n},\mathbf{u}^{n-1},\mathbf{z})}{\partial \mathbf{u}^{n}}\frac{\partial \mathbf{u}^{n}}{\partial \mathbf{z}}+\frac{\partial f(\mathbf{u}^{n},\mathbf{u}^{n-1},\mathbf{z})}{\partial \mathbf{u}^{n-1}}\frac{\partial \mathbf{u}^{n-1}}{\partial \mathbf{z}}\right)\\ &+\sum_{n=1}^{N_t}\lambda_n^{T}\left(\frac{\mathbf{R}(\mathbf{u}^{n},\mathbf{u}^{n-1},\mathbf{z})}{\partial \mathbf{z}}+\frac{\mathbf{R}(\mathbf{u}^{n},\mathbf{u}^{n-1},\mathbf{z})}{\partial \mathbf{u}^{n}}\frac{\partial \mathbf{u}^{n}}{\partial \mathbf{z}}+\frac{\mathbf{R}(\mathbf{u}^{n},\mathbf{u}^{n-1},\mathbf{z})}{\partial \mathbf{u}^{n-1}}\frac{\partial \mathbf{u}^{n-1}}{\partial \mathbf{z}}\right)=0.\end{aligned} \tag{3.2.9}$$

Eq.3.2.9 is satisfied if the following conditions are met:

Final Time Step

$$\frac{\partial f^N(\mathbf{u}^N, \mathbf{u}^{N-1}, \mathbf{z})}{\partial \mathbf{u}^N} + \lambda_N^T \frac{\mathbf{R}^N(\mathbf{u}^N, \mathbf{u}^{N-1}, \mathbf{z})}{\partial \mathbf{u}^N} = 0, \tag{3.2.10}$$

n-th Time Step

$$\begin{aligned} &\frac{\partial f^n(\mathbf{u}^n, \mathbf{u}^{n-1}, \mathbf{z})}{\partial \mathbf{u}^n} + \lambda_n^T \frac{\mathbf{R}^n(\mathbf{u}^n, \mathbf{u}^{n-1}, \mathbf{z})}{\partial \mathbf{u}^n} \\ &+ \frac{\partial f^{n+1}(\mathbf{u}^n, \mathbf{u}^{n-1}, \mathbf{z})}{\partial \mathbf{u}^{n+1}} + \lambda_{n+1}^T \frac{\mathbf{R}^{n+1}(\mathbf{u}^n, \mathbf{u}^{n-1}, \mathbf{z})}{\partial \mathbf{u}^{n+1}} = 0. \end{aligned} \tag{3.2.11}$$

The Lagrange multipliers satisfying stationary conditions Eq.3.2.10 and Eq.3.2.11 are found by solving Eq.3.2.12 and Eq.3.2.13.

Final Time Step

$$\lambda_N^T = -\left[\frac{\mathbf{R}^N(\mathbf{u}^N, \mathbf{u}^{N-1}, \mathbf{z})}{\partial \mathbf{u}^N}\right]^{-1} \left(\frac{\partial f^N(\mathbf{u}^N, \mathbf{u}^{N-1}, \mathbf{z})}{\partial \mathbf{u}^N}\right) \tag{3.2.12}$$

n-th Time Step

$$\begin{aligned} \lambda_n^T = &-\left[\frac{\mathbf{R}^n(\mathbf{u}^n, \mathbf{u}^{n-1}, \mathbf{z})}{\partial \mathbf{u}^n}\right]^{-1} \\ &\left(\frac{\partial f^n(\mathbf{u}^n, \mathbf{u}^{n-1}, \mathbf{z})}{\partial \mathbf{u}^n} + \frac{\partial f^{n+1}(\mathbf{u}^{n+1}, \mathbf{u}^n, \mathbf{z})}{\partial \mathbf{u}^{n+1}} + \lambda_{n+1}^T \frac{\mathbf{R}^{n+1}(\mathbf{u}^{n+1}, \mathbf{u}^n, \mathbf{z})}{\partial \mathbf{u}^{n+1}}\right) \end{aligned} \tag{3.2.13}$$

Given the vector of Lagrange multipliers λ_n, the contribution of time cycle n to the gradient of the objective function is computed as follows:

$$\frac{df}{d\mathbf{z}} = \frac{\partial f(\mathbf{u}^n, \mathbf{u}^{n-1}, \mathbf{z})}{\partial \mathbf{z}} + \sum_{n=1}^{N_t} \lambda_n^T \left(\frac{\partial \mathbf{R}(\mathbf{u}^n, \mathbf{u}^{n-1}, \mathbf{z})}{\partial \mathbf{z}}\right) \tag{3.2.14}$$

Similarly, the gradient of any nonlinear constraint function with respect to the vector of design variables $\mathbf{z}$ is computed using the method of Lagrange multipliers presented in the *Parabolic* section.

3.2.2 Augmented Lagrangian

The augmented Lagrangian method is applied to solve simulation-based design problems with a large number of nonlinear constraints. Consider an optimization problem that seeks to minimize an objective function $\sum_{l=1}^{N_f} f_l(\mathbf{u}, \mathbf{z})$ with PDE constraint $\mathbf{R}(\mathbf{u}, \mathbf{z}) = 0$ and vector of nonlinear inequality constraints $\mathbf{g}(\mathbf{u}, \mathbf{z})$. The optimization problem under consideration can be formulated as:

$$\begin{aligned} \min_{\mathbf{z} \in \mathbb{R}^{N_\mathbf{z}}} \quad & \sum_{l=1}^{N_f} f_l(\mathbf{u}, \mathbf{z}) \\ \text{s.t.} \quad & \mathbf{R}(\mathbf{u}, \mathbf{z}) = 0 \\ & g_j(\mathbf{u}, \mathbf{z}) \leq 0, \ j = 1, \ldots, N_g \\ & \underline{z}_i \leq z_i \leq \bar{z}_i, \ i = 1, \ldots, N_z, \end{aligned} \tag{3.2.15}$$

where N_f is the number of objective functions and N_g is the number of nonlinear constraints. The optimization problem introduced in Eq.3.2.15 becomes computationally intractable if the nonlinear inequality constraints g_j are not properly managed. Indeed, at a minimum, the number of calls made to the multi-physics simulator at each major optimization iteration k equals $1 + N_g$, where each call to the multi-physics simulator requires solving a large linear system of equations. A major optimization iteration is defined herein as the iteration responsible for updating the design variables.

The Morphorm software implements an augmented Lagrangian approach to manage simulation-based optimization problems with a large number of nonlinear constraints, e.g., one or more nonlinear constraints at each material point. At each major optimization iteration k, a sequence of optimization problems given by:

$$\begin{aligned} \min_{\mathbf{z}\in\mathbb{R}^{N_\mathbf{z}}} \quad & \sum_{l=1}^{N_f} f_l\left(\mathbf{u},\mathbf{z}\right) + \frac{1}{N_g}\sum_{j=1}^{N_g}\left[\gamma_j^{(k)}\hat{g}_j\left(\mathbf{u},\mathbf{z}\right) + \frac{\mu_j^{(k)}}{2}\hat{g}_j\left(\mathbf{u},\mathbf{z}\right)^2\right] \\ \text{s.t.} \quad & \mathbf{R}\left(\mathbf{u},\mathbf{z}\right) = 0 \\ & \underline{z}_i \le z_i \le \bar{z}_i,\ i = 1,\ldots,N_z, \end{aligned} \tag{3.2.16}$$

where

$$\hat{g}_j\left(\mathbf{u},\mathbf{z}\right) = \left(g_j\left(\mathbf{u},\mathbf{z}\right), -\frac{\gamma_j^{(k)}}{\mu_j^{(k)}}\right), \tag{3.2.17}$$

$$\gamma_j^{(k+1)} = \gamma_j^{(k)} + \mu_j^{(k)}\hat{g}_j\left(\mathbf{u},\mathbf{z}\right), \tag{3.2.18}$$

$$\mu_j^{(k+1)} = \left(\alpha\mu_j^{(k)}, \mu_{max}\right),\ \alpha > 1. \tag{3.2.19}$$

The augmented Lagrangian problem Eq.3.2.16 is solved until the convergence criteria are met. The parameters $\gamma_j^{(k)}$ and $\mu_j^{(k)}$ are the Lagrange multipliers and scalar penalty values, respectively, associated with the nonlinear inequality constraints $g_j^{(k)}$.

3.3 Criteria

3.3.1 General

The *General* subsection describes the optimization criteria that are indenpendent of the *governing physical equations*. Therefore, these criteria can be used in a simulation-driven design problem, regardless of the governing physical equations. Table 3.3.1 lists all the general optimization criteria supported in the Morphorm software.

Table 3.3.1: General optimization criteria

Type	Description
mass	optimizes the mass of a system
volume	optimizes the volume of a system
p-norm	optimizes the p-norm of a single- or multi-component quantity of interest
state misfit	optimizes the misfit between the targeted and simulated states
state response	optimizes the state on one or more surfaces
mass properties	optimizes the mass properties of a system: mass, center of gravity, and moments of inertia
augmented Lagrangian	applies the augmented Lagrangian method to model local constraints

Mass

The *mass* criterion seeks to optimize the mass of a body Ω. The mass criterion is defined as:

$$\text{mass}(\mathbf{z}) = \int_{\Omega} z\rho_{mass}\, d\Omega, \tag{3.3.1}$$

where ρ_{mass} is the mass density of the material, $\mathbf{z}$ is the vector of design variables describing the material layout, and z is the projected design variables on an element.

Volume

The *volume* criterion seeks to optimize the volume of a body Ω. The volume criterion is used to control the amount of material used to create an optimized configuration. The volume criterion is defined as:

$$\text{volume}(\mathbf{z}) = \int_{\Omega} z\, d\Omega, \tag{3.3.2}$$

where $\mathbf{z}$ is the vector of design variables describing the material layout and z is the projected design variables on an element.

State Misfit

The *state misfit* criterion seeks to match a target state response. The state misfit criterion is defined as:

$$\text{state-misfit}(\mathbf{u}) = \sum_{i=1}^{N_u} \left(\frac{u_i}{u_i^{\star}} - 1.0 \right)^p, \tag{3.3.3}$$

where $\mathbf{u}$ is the vector of state variables, i.e., solution to the governing physical equations, $u_i^{\star}$ is the i-th target state, u_i is the state solution at the i-th measurement point, and $p \geq 1$ is a real number. The default value for p is set to *2.0*.

State Reponse

The *state response* criterion seeks to optimize the state on boundary $\Gamma_{\hat{u}} \subset \Gamma$, where Γ is the boundary of a body Ω. The state response criterion is defined as:

$$\text{state-response}(\mathbf{u}) = \int_{\Gamma} \mathbf{1}_{\Gamma_{\hat{u}}} \mathbf{u}\, d\Gamma \tag{3.3.4}$$

where $\mathbf{u}$ is the vector of state variables. and $\mathbf{1}_{\Gamma_{\hat{u}}} : \Gamma \to \{1, 0\}$ is an indicator function defined as:

$$\mathbf{1}_{\Gamma_{\hat{u}}}(\mathbf{x}) := \begin{cases} 1 & \text{if} \quad \mathbf{x} \in \Gamma_{\hat{u}} \\ 0 & \text{if} \quad \mathbf{x} \notin \Gamma_{\hat{u}} \end{cases}. \tag{3.3.5}$$

Mass Properties

The *mass properties* criterion seeks to match a target set of mass properties. The supported mass properties include the mass, center of gravity, and moments of intertia of a body. The mass of the system is computed via Eq.3.3.1. The center of gravity (CG) of the system is computed via:

$$\mathbf{CG}(\mathbf{z}) = \frac{\int_{\Omega} z\rho_{mass}\mathbf{r}\, d\Omega}{\text{mass}(\mathbf{z})}, \tag{3.3.6}$$

where $\mathbf{r} = (X, Y, Z)$ is the position vector with respect to the origin, ρ_{mass} is the mass density of the material, $\mathbf{z}$ is the vector of design variables describing the material layout, and z is the projected design variables on an element. The mass criterion $\text{mass}(\mathbf{z})$ is defined by Eq.3.3.2. The moment of inertia tensor is computed via:

$$\mathbf{I}(\mathbf{z}) = \int_{\Omega} z\rho_{mass}((\mathbf{r} \cdot \mathbf{r})\mathbf{I}_{3x3} - \mathbf{r} \otimes \mathbf{r})\, d\Omega, \tag{3.3.7}$$

where $\mathbf{I}_{3x3}$ is the 3-by-3 identity tensor.

Match all the mass properties

If the target values for all the mass properties are provided, the optimization problem attempts to remove the dependency of the final design on the coordinate system. The mass and center of gravity properties are computed uisng Eq.3.3.1 and Eq.3.3.6. However, the expression for the moment of inertia follows a different form than the expression in Eq.3.3.7. Indeed, the target moment of inertia tensor $\mathbf{I}_0^\star$ is assumed to have been computed with respect to the origin of the coordinate system, i.e., $(0, 0, 0)$. Therefore, to remove the dependency of the final design on the coordinate system, the moment of inertia tensor is evaluated with respect to the principal frame.

The first step in the process is to use the target center of gravity $\mathbf{CG}^\star$ to evaluate the target inertia tensor about the part center of gravity using the parallel axis theorem as follows:

$$\mathbf{I}_{\texttt{CG}}^\star = \mathbf{I}_{\texttt{0}}^\star - m^\star \left((\mathbf{CG}^\star \cdot \mathbf{CG}^\star)\, \mathbf{I}_{3x3} - \mathbf{CG}^\star \otimes \mathbf{CG}^\star \right), \tag{3.3.8}$$

where $m^\star$ is the target mass and $\mathbf{CG}^\star = \left(CG_x^\star, CG_y^\star, CG_z^\star\right)$ is the target center of gravity, $CG_x^\star$ is the x-component of the target CG, $CG_y^\star$ is the y-component of the target CG, and $CG_z^\star$ is the z-component of the target CG.

The second step in the process is to compute the principal values and principal directions of $\mathbf{I}_{\texttt{CG}}^\star$ as follows:

$$\mathbf{Q}, \mathbf{\Lambda} = \texttt{eigen}(\mathbf{I}_{\texttt{CG}}^\star), \tag{3.3.9}$$

where `eigen` denotes the eigen decomposition of $\mathbf{I}_{\texttt{CG}}^\star$, $\mathbf{Q}$ is a square $n \times n$ matrix whose l-th column is the eigenvector, q_l of $\mathbf{I}_{\texttt{CG}}^\star$ with $l = 1, \ldots, n$, and $\mathbf{\Lambda}$ is a diagonal matrix whose diagonal elements are the eigenvalues $\Lambda_{ll} = \lambda_l$ of $\mathbf{I}_{\texttt{CG}}^\star$. The eigenvalues λ_l are known as the principal moments of inertia in the context of the mass properties criterion. The $\mathbf{Q}$ matrix is later used to rotate the inertia tensor into its principal frame. The predicted inertia tensor $\mathbf{I}(\mathbf{z})$ is computed about the origin $\mathbf{x}_0 = (0, 0, 0)$; however, the predicted inertia tensor is then shifted and rotated via:

$$\hat{\mathbf{I}}(\mathbf{z}) = \mathbf{Q} \cdot \left(\mathbf{I}(\mathbf{z}) - \text{mass}(\mathbf{z}) \left(\mathbf{CG}^\star \cdot \mathbf{CG}^\star \right) \mathbf{I}_{3x3} - \mathbf{CG}^\star \otimes \mathbf{CG}^\star \right) \tag{3.3.10}$$

so that it can be consistent with the target inertia tensor. The predicted moment of inertia tensor $\mathbf{I}(\mathbf{z})$ is computed using Eq.3.3.7 and the predicted mass is computed using Eq.3.3.1. Notice that Eq.3.3.10 uses the predicted mass to compute the shifted and rotated inertia tensor $\hat{\mathbf{I}}(\mathbf{z})$ rather than the target mass $m^\star$.

The final step is to use Eq.3.3.10 to evaluate the misfit in the principal moments of inertia via:

$$\sum_{a=1} w_a^{\hat{I}} \times \left(\frac{\hat{I}_{aa}(\mathbf{z})}{I_a^\star} - 1.0 \right)^2, \text{for } a \in \{1, 2, 3\}, \tag{3.3.11}$$

where $w_a^{\hat{I}} > 0$ are scalar weights, $I_a^\star$ is the a-th component of the target inertia tensor. The off-diagonal components of the principal inertia tensor, Eq.3.3.11, should be zero since the evaluation is done with respect to the principal axes. To achieve this goal, the off-diagonal components of the principal inertia tensor are penalized and normalized with respect to the smallest target principal inertia, i.e., $\min\left(\Lambda_{\ell\ell}\right)$ for $l \in \{1, 2, 3\}$, as follows:

$$\sum_{\alpha} w_\alpha^{\hat{I}} \times \left(\frac{\hat{I}_\alpha(\mathbf{z})}{\min\left(\lambda_1, \lambda_2, \lambda_3\right)} \right)^2, \text{for } \alpha \in \{(1,2), (1,3), (2,3)\}, \tag{3.3.12}$$

where $w_\alpha^{\hat{I}} > 0$ are the scalar weights for the off-diagonal components. Notice the use of a multi-index notation in Eq.3.3.12 in the summation over the off-diagonal components of the principal moments of inertia tensor. Finally, Eq.3.3.11 and Eq.3.3.12 are valid for two-dimensional problems.

Given the definitions for the mass properties subcriteria, the *mass properties* criterion is defined as:

$$\begin{aligned} \text{mass-properties}(\mathbf{z}) = w^m \times \left(\frac{m(\mathbf{z})}{m^\star} - 1.0 \right)^2 + \sum_{a=1}^{d} w_a^{\texttt{CG}} \times \left(\frac{CG_a(\mathbf{z}) - CG_a^\star}{\chi_a} \right) \\ + \sum_{a=1}^{d} w_a^{\hat{I}} \times \left(\frac{\hat{I}_{aa}(\mathbf{z})}{I_a^\star} - 1.0 \right)^2 + \sum_{\alpha=1}^{N_\alpha} w_\alpha^{\hat{I}} \times \left(\frac{\hat{I}_\alpha(\mathbf{z})}{\min\left(\mathbf{\Lambda}_{ll}\right)} \right)^2 \end{aligned} \tag{3.3.13}$$

where $d \in \{1, 2, 3\}$ denotes the spatial dimension, N_α is the number of off-diagonal components in the inertia tensor, $w_\alpha^{\hat{I}} > 0$ are scalar weights, $w^m > 0$ is a scalar weight, $w_a^{\texttt{CG}} > 0$ are scalar weights, and χ_a are the components of the extent vector. The extent vector χ holds the extent of the domain in the respective coordinate directions.

Match a subset of the mass properties

If a subset of target mass properties are specified, the mass and center of gravity subcriteria follow the expressions in Eq.3.3.13. However, only the requested target properties are considered in the evaluation of the mass properties criteria. The expression for the moment of inertia tensor differs from the one used in Eq.3.3.13 since only a subset of the mass properties are provided. Thus, the expression used to evaluate the misfit in the inertia properties is defined as:

$$\sum_{m=1}^{N_I} w_m^I \times \left(\frac{I_m(\mathbf{z})}{I_m^\star} - 1.0 \right)^2 \tag{3.3.14}$$

where N_I is the number of target inerta tensor components and the $I_m(\mathbf{z})$ are the components of the predicted inertia tensor, which are computed via Eq.3.3.7.

Augmented Lagrangian

The *augmented Lagrangian* seeks to enforce a large number of constraints efficiently to minimize the number of linear solves required to compute the gradient. The augmented Lagrangian criterion is defined as:

$$\text{augmented-lagrangian}(\mathbf{u}, \mathbf{z}) = \int_\Omega \frac{1}{N_g} \sum_{j=1}^{N_g} \left[\gamma_j^{(k)} \hat{g}_j(\mathbf{u}, \mathbf{z}) + \frac{\mu_j^{(k)}}{2} \hat{g}_j(\mathbf{u}, \mathbf{z})^2 \right] d\Omega, \tag{3.3.15}$$

where $\mathbf{z}$ is the vector of design variables describing the material layout and $\mathbf{u}$ is the vector of state variables. $\hat{g}_j(\mathbf{u}, \mathbf{z})$, $\gamma_j^{(k)}$, and $\mu_j^{(k)}$ are evaluated using Eq.3.2.17, Eq.3.2.18, and Eq.3.2.19, respectively. Notice that the constraint $\hat{g}_j(\mathbf{u}, \mathbf{z})$ can take on many forms, e.g., von Mises stress, components of the stress tensor, thermal flux, and more.

P-Norm

The *p-norm* criterion seeks to optimize the p-norm of a single- or multi-component quantity of interest over the volume Ω. The p-norm criterion is defined as:

$$\text{p-norm}(\mathbf{u}, \mathbf{z}) = \int_\Omega QoI(\mathbf{u}, \mathbf{z})^p d\Omega, \tag{3.3.16}$$

where $\mathbf{z}$ is the vector of design variables describing the material layout, $\mathbf{u}$ is the vector of state variables, $p > 0$ is a scalar value and $QoI(\mathbf{u}, \mathbf{z})$ is a quantity of interests. Table 3.3.2 lists the quantities of interest that can be used with the p-norm criterion.

Table 3.3.2: Quantities of interest that can be used with the p-norm criterion.

Type	Description
von Mises	von Mises stress
stress component(s)	components of the stress tensor
thermal flux	thermal flux
electrical flux	electrical flux

3.3.2 Physics-Based

This section presents the criteria which usage depend on the governing equations being simulated in the optimization problem.

Mechanical

Table 3.3.3 lists the criteria that can be used when simulating mechanical physics, including multi-physics simulations modeling mechanical environments. The criteria listed in Table 3.3.3 can be used as objectives or constraints in a simulation-based optimization study.

Table 3.3.3: Supported criteria with elastostatics physics

Type	Description
elastic energy	optimizes the elastic energy

Elastic Energy

The *elastic energy* criterion seeks to optimize the elastic energy of an elastic body Ω. The elastic energy criterion is defined as:

$$\text{elastic-energy}(\mathbf{u}, \mathbf{z}) = \int_{\Omega} k^{u}_{ij}(\mathbf{z}) u_i u_j \, d\Omega, \tag{3.3.17}$$

where $k^{u}_{ij}(\mathbf{z})$ is the element stiffness matrix with units of force over length and u_i is the i-th displacement with units of length. The indices $i, j = 1, \ldots, d$, where $d \in \{1, 2, 3\}$ denotes the spatial dimension. The displacement vector $\mathbf{u}$ implicitly depends on the vector of design variables $\mathbf{z}$.

Thermal

Table 3.3.4 lists the criteria that can be used when simulating thermal physics, including multi-physics simulations modeling thermal environments. The criteria in Table 3.3.4 can be used as objectives or constraints in a simulation-based optimization study.

Table 3.3.4: Supported criteria with thermostatics physics

Type	Description
thermal energy	optimizes the thermal energy

Thermal Energy

The *thermal energy* criterion seeks to optimize the thermal energy of a body Ω. The thermal energy criterion, $f^{E_\theta}(\theta(\mathbf{z}), \mathbf{z})$, is defined as:

$$\text{thermal-energy}(\theta, \mathbf{z}) = \int_{\Omega} k^{\theta}(\mathbf{z}) \theta^2 \, d\Omega, \tag{3.3.18}$$

where k^{θ} is the thermal conductivity matrix with units of power over temperature and θ is the temperature with units of temperature. The temperature implicitly depends on the design variables $\mathbf{z}$.

Thermal-Mechanical

Table 3.3.3 lists the criteria that can be used when simulating thermal-mechanical physics The criteria in Table 3.3.5 can be used as objectives or constraints in a simulation-based optimization study.

Table 3.3.5: Supported criteria with coupled thermal-mechanical physics

Type	Description
thermal-elastic energy	optimizes the thermal-elastic energy

Thermal-Elastic Energy

The *thermal-elastic energy* criterion seeks to optimize the thermal and elastic energy. The thermal-elastic energy criterion is defined as:

$$\text{thermal-elastic-energy}(\theta, \mathbf{u}, \mathbf{z}) = w^u \int_\Omega k_{ij}^u(\mathbf{z}) u_i u_j \, d\Omega + w^\theta \int_\Omega k^\theta(\mathbf{z}) \theta^2 \, d\Omega, \tag{3.3.19}$$

where $w^u \in \mathbb{R}$ and $w^\theta \in \mathbb{R}$ are the scalar weights for the elastic and thermal energy criteria, respectively. $k_{ij}^u(\mathbf{z})$ is the element stiffness matrix with units of force over length, u_i is the i-th displacement with units of length, $k^\theta(\mathbf{z})$ is the thermal conductivity matrix with units of power over temperature, and θ is the temperature with units of temperature. The indices $i, j = 1, \ldots, d$, with $d \in \{1, 2, 3\}$ denoting spatial dimension. The temperature and displacements implicitly depend on the vector of design variables $\mathbf{z}$.

Table 3.3.6: Supported criteria with electrical physics

Type	Description
electric power	optimizes the electrical power

Electrical

Table 3.3.6 lists the criteria that can be used when simulating electrical physics, including multi-physics simulations modeling electrical environments. The criteria in Table 3.3.6 can be used as objectives or constraints in a simulation-based optimization study.

Electric Power

The *electric power* criterion seeks to maximize the electric power output of an electrical device. The electric power criterion is defined as:

$$\text{electric-power}(\psi, \mathbf{z}) = \int_\Omega J(\psi, \mathbf{z}) \psi \, d\Omega, \tag{3.3.20}$$

where $J(\psi, \mathbf{z})$ is the current density with units of power over volume and ψ is the electric potential with units of volts. The electric potantial implicitly depends on the vector of design variables $\mathbf{z}$.

3.4 Topology Optimization

Topology optimization is a mathematical method used to optimize the material layout of a physical system, or component, given a set of mathematical objective and constraint functions. Topology optimization is not shape optimization, which is defined here as a mathematical method used to optimize the parametric shape parameters that form the geometry. In topology optimization, the optimizer is free to choose any material layout within the design space that satisfies the design objectives and constraints. In contrast, shape optimization methods, operate on a restricted set of geometric features, i.e. shape parameters, that define the geometry.

A topology optimization problem can be formulated as follows:

$$\begin{aligned} \min_{\mathbf{z} \in \mathbb{R}^{N_z}} \quad & \sum_{i=1}^{N_f} f_i(\mathbf{u}, \mathbf{z}) \\ \text{s.t.} \quad & g_j(\mathbf{u}, \mathbf{z}) \leq 0 \quad \text{with } j = 1, \ldots, N_g \\ & \underline{z}_i \leq z_i \leq \bar{z}_i, \; i = 1, \ldots, N_z \end{aligned} \tag{3.4.1}$$

The general topology optimization problem introduced in Eq.3.4.1 includes:

- N_f objective functions $f_i(\mathbf{u}, \mathbf{z})$ with $i = 1, \ldots, N_f$. The objective functions represent the quantities that are being minimized, or maximized, to improve the performance of the physical system.

- The material layout is represented with the vector of design variables $\mathbf{z}$. The design variable field is defined by a pseudo-density at each material location in the case of density-based topology optimization or by a level-set field in the case of level-set topology optimization.
- N_g constraint functions $g_j(\mathbf{u}, \mathbf{z})$. The constraint functions represent the performance requirements that the optimized system must meet.
- The quantities $\underline{z}_i$ and $\bar{z}_i$ in Eq.3.4.1 are the i-th lower and upper bounds for the the design variable z_i, where N_z is the number of design variables

Evaluating that vector of state variables $\mathbf{u} \in \mathbb{R}^{N_u}$ requires solving partial differential equations using a computational method for solving partial differential equations numerically, e.g., the finite element method, since these equations do not have a known analytical solution. Here, N_u is the number of state variables.

3.4.1 Material Description

Ideally, in a topology optimization problem, the design variables should be modeled as a discrete variable that only can take on a zero or one value at a material point. In most two-phase structural topology optimization problems, a value of one indicates the existance of material while a value of zero denotes the abscence of material. In some topology optimization problems, each phase may represent a material, e.g., fluid physics. Discrete optimization methods could be employed to solve Eq.3.4.1. However, as the number of design variables increases, discrete optimization methods are not the optimization method of choice to solve topology optimization problems. To bypass this limitation, a continuum design variable description is employed to model the material layout within the allowable design space. This approach, combined with the *adjoint method*, enables the use of gradient-based optimization methods to solve Eq.3.4.1. Gradient-based optimization methods have been shown to be more effective in solving topology optimization problems with a large number of design variables than discrete optimization methods.

Density Method

A critical aspect of density-based topology optimization methods is the selection of the material interpolation function, which is used to steer the optimizer towards a "0-1" design solution. In density-based structural topology optimization problems, a pseudo-density takes on a value within the following range of values: $0 \leq \underline{z}_i \leq z_i \leq 1$, where a value of 0 denotes the absence of material and a value of 1 denotes the existence of material.

The Morphorm software employs a modified Solid Isotropic Material Penalization (SIMP) material interpolation scheme:

$$\tilde{z}_i = z_i^{low} + (1 + z_i^{low})\hat{z}_i^p, \tag{3.4.2}$$

where $\tilde{z}_i$ is the interpolated pseudo-density, $\hat{z}_i$ is the *filtered* pseudo-density, z_i^{low} is the minimum value the pseudo-density can take. The z_i^{low} parameter is used to prevent the linear system of equations from becoming singular. The parameter $p > 0$ is known as a penalization factor, which is set to 3 by default. In addition, *filters* are used to avoid numerical artifacts that result from the discretization of the vector of pseudo-densities $\mathbf{z}$ with an unstable finite element formulation. Filters also provide a mechanism to implicitly enforce a minimum feature size on the structural features. While filters do not completely eliminate the mesh-dependency issue, it greatly helps control it.

3.4.2 Filters

Kernel Filter

A linear kernel filter [Bourdin] is mathematically defined as:

$$F_{ij} = \max\left(0, 1 - \frac{d(i,j)}{R}\right), \tag{3.4.3}$$

where R is the filter radius, $d(i,j)$ is the distance between pseudo-densities z_i^m and z_j^m for candidate material m. The filtered pseudo-density $\hat{z}_i^m$ for candidate material m is computed as follows:

$$\hat{z}_j^m = \sum_{i=1}^{N_{pts}} = w_{ij} z_i^m, \tag{3.4.4}$$

where N_{pts} denotes the number of pseudo-densities inside the filter radius. The weights w_{ij} are computed via:

$$w_{ij} = \frac{F_{ij}}{\sum_{k \in \mathcal{N}_j} F_{kj}}, \tag{3.4.5}$$

where $\mathcal{N}_j = \{z_i^m \colon d(i,j) \leq R\}$ is the neighborhood of pseudo-densities inside the filter radius R with respect to pseudo-density z_j^m, which includes the pseudo-densities at the boundary of the search radius. Eq.3.4.3 can take on other forms, i.e., the kernel filter does not need to be linear.

Helmholtz Filter

The Helmholtz filter is another approach for enforcing a minimum feature size constraint in topology optimization problems. Traditionally, the Helmholtz filter has been formulated as the minimization of the potential:

$$\Pi(\hat{\mathbf{z}}) = \frac{1}{2} \int_\Omega \ell_\Omega^2 \|\nabla \hat{z}\|^2 \, d\Omega + \frac{1}{2} \int_\Omega (z - \hat{z})^2 \, d\Omega, \tag{3.4.6}$$

where ℓ_Ω is a length scale parameter. The second integral above aims to keep the filtered design variable $\hat{z}$ close to the unfiltered design variable z. Meaning, the filtered design variable should not be significantly different than the unfiltered design variable. However, the unfiltered design variable can be highly oscillatory, which the first integral in Eq.3.4.6 aims to control. The compromise between these two goals is regulated by the lenght scale parameter ℓ_0.

Minimizing Eq.3.4.6 with respect to the filtered design variable $\hat{z}$ and requiring $\delta\Pi(\hat{z}; \delta\hat{z}) = 0 \; \forall \; \delta\hat{z}$ gives the standard Helmholtz filter [Lazarov and Sigmund]:

$$\begin{aligned} &- \ell_\Omega^2 \Delta \hat{z} + \hat{z} - z = 0 \quad \text{in } \Omega \\ &\text{with:} \quad \nabla \hat{z} \cdot \mathbf{n} = 0 \quad \text{on } \Gamma, \end{aligned} \tag{3.4.7}$$

where $\mathbf{n}$ is the outward normal unit vector to boundary Γ. iOne drawback of the Helmholtz filter formulation in Eq.3.4.6 is that it does not penalize placement of material along the boundaries of the design. This causes the Helmholtz filter to favor optimized designs with boundaries coinciding with the the boundaries of the allowable design space. This undesired behavior is know as the "stick" effect. Luckily, this problem can be mitigated by assigning a cost to material placed along the boundaries of the allowable design space [Wallin *et al.*]. Therefore, a boundary integral is added to Eq.3.4.6, which gives:

$$\tilde{\Pi}(\hat{\mathbf{z}}) = \frac{1}{2} \int_\Omega \ell_\Omega^2 \|\nabla \hat{z}\|^2 \, d\Omega + \frac{1}{2} \int_\Omega (z - \hat{z})^2 \, d\Omega + \frac{1}{2} \int_\Gamma \ell_\Gamma \hat{z}^2 d\Gamma, \tag{3.4.8}$$

where Γ is the boundary of the design volume, i.e., allowable design space, Ω. The parameter ℓ_Γ is the surface length scale parameter used to penalize placement of material along the boundaries of the allowable design space [Wallin *et al.*]. Minimizing Eq.3.4.8 with respect to the filtered design variable and requiring $\delta\Pi(\hat{z}; \delta\hat{z}) = 0 \; \forall \; \delta\hat{z}$ gives:

$$\delta\tilde{\Pi}(\hat{\mathbf{z}}) = - \int_\Omega \ell_\Omega^2 \Delta\hat{z} \delta\hat{z} d\Omega - \int_\Omega (z - \hat{z}) \delta\hat{z} d\Omega + \int_\Gamma (\ell_\Omega^2 \nabla\hat{z} \cdot \mathbf{n} + \ell_\Gamma \hat{z}) \delta\hat{z} d\Gamma = 0. \tag{3.4.9}$$

Eq.3.4.9 should be fulfilled for arbitrary variations of $\delta\hat{z}$, which gives the Robin boundary condition:

$$\ell_\Omega^2 \nabla\hat{z} \cdot \mathbf{n} = -\ell_\Gamma \hat{z} \quad \text{on } \Gamma. \tag{3.4.10}$$

Instead of solving Eq.3.4.7 with a homogeneous Neumann boundary condition on Γ, Eq.3.4.9 is solved with the Robin boundary condition defined in Eq.3.4.10. Notice that when the surface length scale parameter goes to zero, i.e., $\ell_\Gamma \to 0$, Eq.3.4.7 is recovered. In contrast, placing material along the external boundaries is penalized as $\ell_\Gamma \to \infty$. Thus, placement of material along the external boundaries of the design is discouraged.

Heaviside Projection

In addition to the material interpolation functions and the filters, density-based topology optimization problems may require the use of a projection method to steer the optimizer towards a "0-1" design solution. The density filter can create transition regions with intermediate pseudo-density values. In order to discourage the creation of these transition regions, the optimizer applies a projection method. Indeed, the Morphorm software applies a heaviside projection function of the form:

$$\hat{\hat{z}}_j^m = \frac{\tanh(\beta\eta) + \tanh(\beta(\hat{z}_j^m - \eta))}{\tanh(\beta\eta) + \tanh(\beta(1-\eta))}, \tag{3.4.11}$$

where $\hat{z}_j^m$ is the j-th filtered pseudo-density for candidate material m. The parameter η governs the pseudo-density threshold at which the projection takes place and β governs the strength of the projection. The $\hat{\hat{z}}_j^m$ is the j-th projected pseudo-density for candidate material m. The parameter η is set to a default value of 0.5 while a continuation scheme is used to update β. The parameter β is incrementally increased at a fixed rate to steer the optimizer towards a "0-1" design solution. When Eq.3.4.11 is enabled, Eq.3.4.2 is recast as:

$$\tilde{z}_i = z_i^{low} + (1 + z_i^{low})\hat{\hat{z}}_i^p i, \tag{3.4.12}$$

where $\hat{\hat{z}}_i^p i$ is the projected filtered pseudo-density and z_i^{low} is the minimum value the projected filtered pseudo-density can take.

3.4.3 Fixed Blocks

In topology optimization problems, the optimizer is allow to add or remove material at every material point within the design domain Ω. In some applications, the user may want to discourage the optimizer from removing material from certain regions/domains due to practical considerations. For instance, a component must be mounted on top of a surface. Thus, the optimizer must be instructed to avoid removing material from the mounting surface and surrounding areas. The fixed block feature enables specification of non-optimizable regions in the design domain. This information is pass to the optimizer so that it does not remove material from the non-optimizable regions.

BIBLIOGRAPHY

[Aug23] Pierre Auger. Sur les rayons b secondaires produits dans un gaz par des rayons x. *CR Acad. Sci.(F)*, 177:169, 1923.

[BRGC86] G Baccarani, M Rudan, R Guerrieri, and P Ciampolini. Physical models for numerical device simulation. In *Process and device modeling*, pages 107–158. 1986.

[BB78] D Bednarczyk and J Bednarczyk. The approximation of the fermi-dirac integral f12(n). *Physics letters A*, 64(4):409–410, 1978.

[Bet91] Hans Albrecht Bethe. Theory of the boundary layer of crystal rectifiers. In *Semiconductor Devices: Pioneering Papers*, pages 387–399. World Scientific, 1991.

[BPP15] Pavel Bochev, Mauro Perego, and Kara Peterson. Formulation and analysis of a parameter-free stabilized finite element method. *SIAM Journal on Numerical Analysis*, 53(5):2363–2388, 2015.

[Bou01] Blaise Bourdin. Filters in topology optimization. *International journal for numerical methods in engineering*, 50(9):2143–2158, 2001.

[BH82] Alexander N Brooks and Thomas JR Hughes. Streamline upwind/petrov-galerkin formulations for convection dominated flows with particular emphasis on the incompressible navier-stokes equations. *Computer methods in applied mechanics and engineering*, 32(1-3):199–259, 1982.

[Cal91] Herbert B Callen. *Thermodynamics and an Introduction to Thermostatistics*. John wiley & sons, 1991.

[DHuckel23] Peter Debye and Erich Hückel. On the theory of electrolytes. i. freezing point depression and related phenomena. *Phys. Z*, 24:185–206, 1923.

[Eva22] Lawrence C Evans. *Partial differential equations*. Volume 19. American Mathematical Society, 2022.

[GVL13] Gene H Golub and Charles F Van Loan. *Matrix computations*. JHU press, 2013.

[Gum64] Hermann K Gummel. A self-consistent iterative scheme for one-dimensional steady state transistor calculations. *IEEE Transactions on electron devices*, 11(10):455–465, 1964.

[Hal52] Re N Hall. Electron-hole recombination in germanium. *Physical review*, 87(2):387, 1952.

[Hof13] Hellmut Hofmann. *Das elektromagnetische Feld: Theorie und grundlegende Anwendungen*. Springer-Verlag, 2013.

[Hug03] Thomas JR Hughes. *The finite element method: linear static and dynamic finite element analysis*. Courier Corporation, 2003.

[KWL08] Raseong Kim, Xufeng Wang, and Mark Lundstrom. Notes on fermi-dirac integrals. *arXiv preprint arXiv:0811.0116*, 2008.

[KSDG92] DBM Klaassen, JW Slotboom, and HC De Graaff. Unified apparent bandgap narrowing in n-and p-type silicon. *Solid-State Electronics*, 35(2):125–129, 1992.

[LS11] Boyan Stefanov Lazarov and Ole Sigmund. Filters in topology optimization based on helmholtz-type differential equations. *International journal for numerical methods in engineering*, 86(6):765–781, 2011.

[Lew91] Leonard Lewin. *Structural properties of polylogarithms*. Number 37. American Mathematical Soc., 1991.

[LS88] Chia-Chiao Lin and Lee A Segel. *Mathematics applied to deterministic problems in the natural sciences*. SIAM, 1988.

[MGT+16] Denis Mamaluy, Xujiao Gao, Brian David Tierney, Matthew Marinella, Patrick Mickel, and Brian D. Tierney. Fully-coupled thermo-electrical modeling and simulation of transition metal oxide memristors. Technical Report, Sandia National Lab.(SNL-NM), Albuquerque, NM (United States), 11 2016. URL: https://www.osti.gov/biblio/1331433, doi:10.2172/1331433.

[Mar83] Peter A Markowich. A qualitative analysis of the fundamental semiconductor device equations. *COMPEL-The international journal for computation and mathematics in electrical and electronic engineering*, 2(3):97–115, 1983.

[Mar13] Peter A Markowich. *The stationary semiconductor device equations*. Springer Science & Business Media, 2013.

[MR84] Peter A Markowich and CA Ringhofer. A singularly perturbed boundary value problem modelling a semiconductor device. *SIAM Journal on Applied Mathematics*, 44(2):231–256, 1984.

[Mar89] Alan H Marshak. Modeling semiconductor devices with position-dependent material parameters. *IEEE transactions on electron devices*, 36(9):1764–1772, 1989.

[MSW99] John James Henry Miller, WHA Schilders, and Song Wang. Application of finite element methods to the simulation of semiconductor devices. *Reports on Progress in Physics*, 62(3):277, 1999.

[Nil73] NG Nilsson. An accurate approximation of the generalized einstein relation for degenerate semiconductors. *physica status solidi (a)*, 19(1):K75–K78, 1973.

[NW99] Jorge Nocedal and Stephen J Wright. *Numerical optimization*. Springer, 1999.

[OR00] James M Ortega and Werner C Rheinboldt. *Iterative solution of nonlinear equations in several variables*. SIAM, 2000.

[Pau25] Wolfgang Pauli. Uber den zusammenhang des abschlusses der elektronengruppen im atom mit der komplexstruktur der spektren. *Zeitschrift fur Physik*, 31(1):765–783, 1925.

[Pre07] William H Press. *Numerical recipes 3rd edition: The art of scientific computing*. Cambridge university press, 2007.

[SOK94] D Schroeder, T Ostermann, and O Kalz. Comparison of transport models far the simulation of degenerate semiconductors. *Semiconductor science and technology*, 9(4):364, 1994.

[Sel12] Siegfried Selberherr. *Analysis and simulation of semiconductor devices*. Springer Science & Business Media, 2012.

[SGPotzl84] Siegfried Selberherr, W Griebel, and Hans Pötzl. Transport physics for modeling semiconductor devices. In *Proceedings of the International Conference on Simulation of Semiconductor Devices and Processes*, 133–152. 1984.

[SRJ52] WTRW Shockley and WT Read Jr. Statistics of the recombinations of holes and electrons. *Physical review*, 87(5):835, 1952.

[SLN21] Simon M Sze, Yiming Li, and Kwok K Ng. *Physics of semiconductor devices*. John wiley & sons, 2021.

[VR50] W Van Roosbroeck. Theory of the flow of electrons and holes in germanium and other semiconductors. *The Bell System Technical Journal*, 29(4):560–607, 1950.

[WIAT20] Mathias Wallin, Niklas Ivarsson, Oded Amir, and Daniel Tortorelli. Consistent boundary conditions for pde filter regularization in topology optimization. *Structural and Multidisciplinary Optimization*, 62:1299–1311, 2020.